

## Point-by-point response

### Reply to Review 1:

We are most grateful to Referee 1 for the encouraging comments and constructive suggestions. The Referee pointed out the usefulness of the study in clarifying the issues of particle size dependency on shear stress and possibly atmospheric boundary layer stability. We have now considered the suggestions by the Referee and modified the text accordingly.

*C1) P1, l26: F increases with Q, but it is not simply proportional to it. For a given surface, the so-called 'sandblasting-efficiency' (ratio of F to Q) is usually found to vary with  $u_*$ .*

Existing data suggest that  $Q \sim u_*^3$ , but  $F \sim u_*^n$  and n is not necessary 4. This issue has been clarified in several earlier studies by the first author together with Hua Lu. Different definitions of “saltation bombardment efficiency” exist in the literature, but the Referee is certainly right in stating that F/Q varies with  $u_*$ . Indeed, this has been one of the main conclusions of Shao (2001; 2004). In order not to slow down the pace of introduction, we added a footnote for clarification.

*C2) P2, l45 and 48: correct the years for Kok's publications*

Corrected.

*C3) P2, l62: in Ishizuka et al. (2008) and in this paper,  $u_*$  is calculated over periods of 1'. This is too short to integrate the time-scales of turbulence in the surface layer (Dupont et al., 2019), but presents the advantage of following more closely the variations of the instantaneous wind speed to which saltation responds in quasi real-time. Conversely, Khalfallah et al. (2020) calculated  $u_*$  over longer periods of 16'. The smoothing of the  $u_*$  statistical distribution resulting from this averaging probably explains that they could not detect any notable influence of  $u_*$  on the emission PSD.*

We would agree with the referee. In boundary-layer studies, using the flux-gradient relationship to estimate friction velocity from wind profile requires relatively long time averaging, typically 15 to 30 minutes, and averaging over 1 min would not be enough. But for saltation, 1-minute average gives the advantage to examine the fluctuations of saltation and dust emission. To include turbulence in the study of dust emission particle size is an important aspect of our paper. We do not know whether Khalfallah et al. (2020) would reach a different conclusion if  $u_*$  is averaged shorter. Dr. Alfaro informed us that they are reexamining their data. Discussions added to the text.

*C4) P3 l64: JADE (not JADA)*

Thanks. Corrected.

*C5) P4 l88: In sedimentology, the texture of a soil is defined from the size-distribution of its particles after full dispersion. So, the soil is sandy loam.*

Thanks for both Referees pointing out this. The first author has misunderstood this for years. It is now corrected.

*C6) P6, Fig. 4a: In the insert, the same color code as in the rest of the figure could be used to differentiate Event 10 from Event 11.*

Changes made as suggested. Thanks.

*C7) P6, l144: 'do not substantially differ'. What does this mean?*

This line is deleted at this location, but we have added a substantial section to discuss the problem of data uncertainty.

*C8) P8, l177: what are the implications of the fact that the distribution of  $\bar{v}_A t$  is skewed to smaller values?*

This suggests the LES results of Klose et al. (2014) seem to be qualitative reasonable.

*C9) P10, l208: experiments 'were' . . .*

Changed. Thanks.

*C10) P113, l229-235: Please rewrite this part to avoid repetitions and clumsy formulations.*

We tried to improve, but are not sure how to write much better.

## Reply to Review 2:

We are most grateful to Referee 2 for his/her review and helpful comments, which we have addressed in the revision.

First of all, we fully agree with the referee, that this paper is part of the ongoing debate and we definitely need more experimental data to fully solve the question. This paper points to the PSD dependency on  $u_*$  and atmospheric boundary layer stability. In fact, the Japanese team (Ishizuka et al.) have more recently collected data in Mongolia. We will look into that dataset, once it is ready. But more time is needed to quantity check, preprocess and homogenize the data.

*C1): Introduction: The introduction is very well written, concise and gives a clear idea of the scientific context. lines 41-42 (and also mentioned on line 144-145): I agree with the authors that dust-airborne PSD measured very close to the surface can probably be assimilated to dust-emission PSD by assuming that the difference of the particle diffusivity compared at that of other scalar (and thus, its dependency on particle diameter) can be neglected. However, because this assumption is an important point of the paper, it deserves to be better discussed, especially because there are few experimental data on particle diffusivity, especially for small particles, and that most of the information we have come from models. In the same way, since the authors indicate that size-resolved dust fluxes were measured during JADE (line 67) a comparison between dust-airborne PSD and dust-flux PSD should be added to support this assumption, at least in the supplement. line 49: the only reference to the Pisso et al., 2019 's paper is not sufficient to support the statement that "The proposed emission-dust PSD is frequently used in dust models". 152: replace airborne-dust PSD by "dust flux PSD" or "emission dust PSD"*

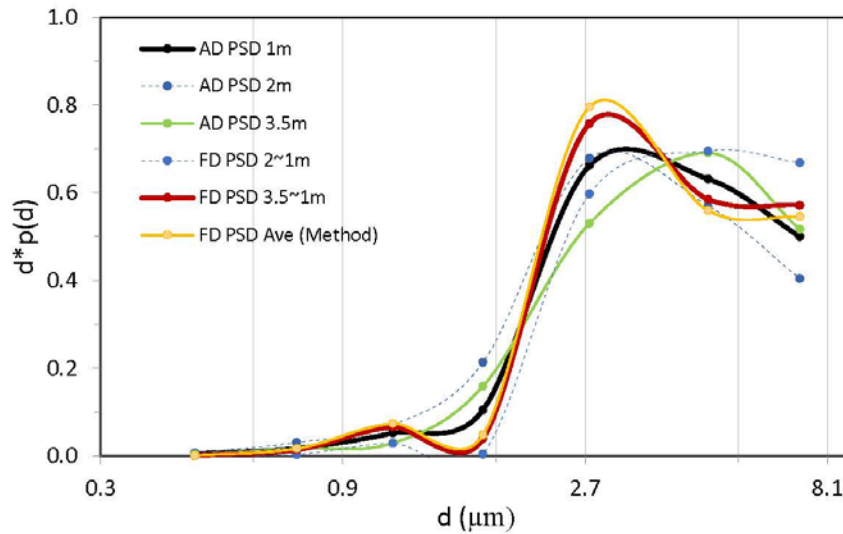
These are substantial suggestions. The Referee pointed out the need for discussion of heavy particle diffusivity in turbulent flows. This is a large topic in itself and studies dedicated to the topic are numerous. The Referee is right in saying that "there are few experimental data on particle diffusivity, especially for small particles, and that most of the information we have come from models". To our best knowledge, the understanding of particle diffusivity still rests on the study of Csanady (1963, Turbulent Diffusion of Heavy Particles in the Atmosphere. J. Atmos. Sci. 20, 201–208). His result is that particle eddy diffusivity  $K_p$  is related to eddy diffusivity  $K$  by

$$K_p = K(1 + \beta^2 w_t^2 / \sigma^2)^{-1/2}$$

where  $\beta$  is a coefficient (about 1 to 2),  $w_t$  is particle terminal velocity and  $\sigma$  is the standard deviation of turbulent velocity. The studies of Csanady (1963), Walklate (1987, A random-walk model for dispersion of heavy particles in turbulent air flow. Boundary-Layer Meteorol. 39:175–190) and Wang and Stock (1993, Dispersion of heavy particles by turbulent motion. J Atmos Sci 50:1897–1913) all suggest that  $K_p$  depends on particle size and turbulence intensity. For the particle-size range we consider,  $K_p/K$  is close to 1 for  $\sigma = 0.5$  m/s, and for  $\sigma = 0.1$  m/s, it is still larger than 0.95 (Shao, 2008, Physics and Modelling of Wind Erosion, Fig. 8.12).

However, the variation of airborne-dust PSD in the vertical direction due to transport processes in the atmosphere cannot be ruled out. Plotted here is a comparison of (Event-10 averaged) airborne-dust PSD measured at 1, 2 and 3.5m. Ishizuka et al. (2014) excluded the 2m OPC data, because they do not correlate with the OPC measurements at the other heights. We had another look at the airborne-dust PSD measured at 2m, it does show some differences from those measured at 1m and 3.5m. To reduce uncertainties, we will now exclude the 2m OPC data from the study. The figure shows that the airborne-dust PSD observed at 1m and 3.5m also somewhat differ, with peak particle size shifting from smaller to larger values. We cannot fully explain this difference, but suspect that particle deposition may have played a role. The dependency of deposition velocity on particle size in the size range of 1 to 10  $\mu\text{m}$  is rather complex (Zhang and Shao 2014, A new parameterization of particle dry deposition over rough surfaces. Atmos. Chem. Phys 14, 12429-12440).

We are not aware of direct measurements of emission-dust PSD. A flux-dust PSD is possible, namely, a PSD estimated based on size-resolved dust flux. However, because dust flux is estimated from the vertical gradient of dust concentration, the flux-dust PSD describes basically the dependency of concentration gradient on particle size, not the concentration itself on particle size.



We added this graph to the text and added discussions similar to the above to the text. We have cited more studies, in which invariant emission-dust PSD is used.

2. JADE data line 64: replace JADA by JADE. I know that the JADE experiment has been described in details in various papers, especially in Ishizuka et al., 2008, and does not need to be described again. However, the presentation of the data in this paper is too short: for example, it is never indicated that OPCs measured number concentrations that are further converted into mass concentrations assuming spherical particles of density= 2380 kg m<sup>-3</sup>. In the same way, Ishizuka et al. (2014) mentioned that the measurements for the bin 0.3-0.6 μm were not considered because of a significant difference between the two OPCs for this bin. In the present paper, this bin is used and the reason for that should be explained, at least to be consistent with the previous paper. However, it must be noted that this point is not critical for this paper since the contribution of this bin is negligible in mass as shown on figures 3 and 4.

Finally, line 96, it is indicated that no rainfall occurred as a consequence of the cold front crossing but in Ishizuka et al; (2008), it is mentioned that the rain sensor detected several very small precipitation events that have been also observed by the authors. Even if, as mentioned in Ishizuka et al. (2008) the drying of the soil was very rapid, this should be mentioned.

We corrected “JADA” to “JADE”.

Thanks for the insightful comments. There are some issues related to the OPC 0.3-0.6μm size bin if the data are used for dust flux calculations (Shao et al. 2011). For airborne-dust PSD examination, this does not seem to be a problem. The Referee pointed out, this is not a critical issue. We have made no changes in the text in relation to the 0.3-0.6μm size bin.

As discussed above, the 2m-OPC data are now excluded from the analysis. The overall conclusion of the paper remains qualitatively unchanged.

We modified the text to include the description of Ishizuka et al. (2008) regarding possible precipitation. We added some words in this respect to the discussion section.

Figure 1: The measured dust concentrations are very high (several mg m<sup>-3</sup>!) even for event 11. This should be underlined in the text. Indeed, since the authors used airborne-dust PSD and not dust flux PSD, it is necessary to provide arguments showing that the measured dust PSD can be directly linked to dust emission. And such high concentrations of dust strongly suggest that the contribution of advection to the measured dust PSD is probably very limited.

We have added some text as the Referee suggested and also modified the figure. Advection may have contributed to the extremely high concentrations shortly before and after the cool change. These time periods are now excluded from our analysis.

*line 88: reformulate. A soil has only one texture. A formulation such as “The results of the analyze by method A correspond to (or suggest) a loamy sand texture while the results of the analyze by method B. . .” should be better.*

Referee I made the same comment. We have changed the text as the referees have suggested.

*line 91: I appreciate the method consisting to select among various dust events those the best adapted to the objective of the occurred under daytime unstable, while Event-11 under night-time stable, conditions”). I imagine that they were other events among the 12 aeolian events recorded during JADE that occurred also in stable or unstable conditions. Are these events selected because the stability conditions were particularly constant for these two events?*

We agree with the Referee. In the revised paper, we use Events 10 and 11 for detailed case studies but present all events in the new discussion section.

### 3. Results

*Figure 3: we have no idea of the number of points contributing to each  $u^*$  category. This should be added in the legend of the figure; in the same way, no information is provided on the spread of the different points that allow to construct the PSD (standard deviation bars should be added). The authors write “that dust PSDs for Event-10 and -11 considerably differ”: maybe an additional panel reporting the difference between PSD10 and PSD11 for similar  $u^*$  categories could better illustrate these differences in PSD.*

Thanks for this suggestion. We have now substantially reworked on the data. Presented the averages for the entire JADE dataset.

*Figure 4: This figure in which are averaged all heights and all  $u^*$  is important since it clearly shows that the dust and saltation PSD shift between the two events. However, this averaging approach is not well introduced and it should not be obvious for the reader to understand why it is useful and relevant to make such averaging. The paper should explain that. The insert is too small and should be a figure by itself. Same comment concerning standard deviations as for figure 3.*

Thanks for this suggestion. We tried to better explain in the revised version.

*On figure 6, there is a shouldering in the high values for the observed  $u^*$  distribution corresponding to event 11. This suggests that the  $u^*$  PDF could be bimodal for this event. Moreover, the adjusted Gaussian PDF for  $u^*$  does not include this shouldering reducing the variance of the  $u^*$  Gaussian PDF for event 11. This should be discussed. The numerical simulations are interesting and illustrate the sensitivity of the impact kinetic energy to different parameters on which the stability conditions could act. They clearly suggest that larger variances in  $u^*$  PDF, as generally observed in unstable conditions, generate stronger saltation and thus should be responsible for higher production of fine particles.*

In the very earlier phase of Event 11, there are some big  $u_*$  values which produced the “shouldering”. It is not that Event 11 is generally a case with bimodal  $u_*$  values.

### Reply to Review 3:

*I read the manuscript from the perspective of a specialist in wind erosion and dust emission but a generalist to this specific focus of the manuscript. The authors provide a clear, logical development of the focuses of their manuscript on the different bases for explaining particle size distributions of emitted dust and the dependency of airborne dust PSD on atmospheric boundary layer (ABL) stability. The topic is valuable for the community and the work is well presented. However, I am not convinced by the approach used in the manuscript. I think the work in the manuscript omits uncertainty. If that uncertainty were included, I think it may lead to different / alternative conclusions.*

*Therefore, to increase confidence in the results I think the omitted uncertainty must be tackled, in some form or other, before the work can be published. I provide below additional information on this point. I also think that some improvements in the structure of the manuscript will help the reader more easily follow the explanation of the work. In short, I am thoroughly supportive of the work. I think the manuscript needs to be revised to give confidence that the results are indeed detectable and therefore interpretations are robust to the uncertainty. The nature of the revisions I describe below I think, are consistent with a major revision, despite not being too difficult to achieve in a short period of time, if all other things were equal.*

Thanks for Review 3 for the support and the valuable comments. We fully agree, uncertainty analysis is important. In the revised paper, we have made the effort to increase the uncertainty analysis by (1) reworked on the full data set, this substantially increased the sample size; (2) added error bars in some graphs. We did not add error bars to all graphs, because the overlap of the error bars can make the graphs messy; (3) added a discussion section. The qualitative conclusion of the revised paper remains the same as in the earlier version.

#### *Main issues*

*Wind friction velocity uncertainty. In the abstract, it is stated that friction velocity  $u^*$  is a surrogate for surface shear stress and descriptor for saltation bombardment intensity. Line 32 states that “for a given soil, the particle size distribution of dust at emission (emission-dust PSD),  $ps(d)$ , must depend on saltation bombardment or on friction velocity”. The JADE field measured data are used to show that the (finely resolved) particle size distribution is dependent on measured wind friction velocity. In contrast to this approach, it is well known (cf. sediment transport models) that the wind energy available for saltation bombardment is not  $u^*$ , it is the energy  $us^*$ , which remains after wind momentum has been extracted by the roughness ‘canopy’. In other words,  $us^*=u^*.R$  where  $R$  is the partition of drag. Under controlled conditions with homogeneous material, smooth surface (bed) without ripples and the bed reset after each experiment, it may be reasonable to assume that  $R=1$ . However, the authors use field data which, even under the smoothest field conditions are very likely to cause  $R$  not equal to 1. For example, soil has different sized aggregates at the surface, stones occur in the field, plant residue may be fixed to, or lying on, the soil and ripples may occur intermittently during sediment transport (and that is to say nothing of intermittent crusts which may change roughness). The magnitude of  $R<1$  (which may change over time, between events due to change in the roughness ‘canopy’) is the omitted uncertainty in the authors’ methodology.*

*For clarity, I think the authors should state clearly that they are assuming  $u^*=us^*$ . I think the authors must then ideally estimate, or at least approximate, the uncertainty of making that assumption ( $R=1$ ) under field conditions when  $R<1$ . That ‘model’ uncertainty will then manifest as an error on  $u^*$ . When the PSDs are aggregated under this explicit approach, that ‘model’ uncertainty (not to be confused with the standard deviation of  $u^*$  already included by the authors) will demonstrate the extent to which there is a difference in the PSDs which is detectable. Any difference between the PSDs remaining after that ‘model’ uncertainty has been included will have accounted for the dependency of PSD on  $us^*$  and  $R$ .*

*I think the same issue of uncertainty occurs with the relation between the dependency of emission-dust PSD on  $u^*$  and the boundary-layer stability. Where  $u^*$  is based on field measurements, I think it requires the same (as above) expression of uncertainty. As above, this uncertainty is required due to the assumption that  $u^*=us^*$  when field conditions introduce uncertainty. Consequently, the results in the second half of the paper need to be similarly qualified with this uncertainty. The issue is brought to sharp focus by considering Eq. 8 of the manuscript. The sediment transport  $Q$  is related incorrectly to  $u^{*3}$  (Webb et al., 2020). As above, the available energy for transport is  $us^{*3}$ . Whilst there are conditions when  $u^*=us^*$  and therefore  $R=1$ , in the field it is very unlikely that  $R=1$ . In this case, the uncertainty of the ‘model’ assumption  $u^*=us^*$ , needs to be considered ( $R<1$ ). With this additional uncertainty the arising figures and interpretations may need to be re-evaluated.*

We are well aware of the excellent paper by Webb et al. (2020). However, to include the roughness related uncertainties would dramatically complicated the problem and will lead to more uncertainties in an

already complex problem. Having said this, we believe the roughness issue is not so relevant to this study, because the JADE site was practically bare. What could influence roughness length are ripples. Using field measurements to detect changes in surface roughness (e.g. ripples) is difficult and in JADE we did not measure ripple changes. As saltation flux used in this study is measured, we do not see how the roughness correction comes into play. What can be done are probably some sensitivity tests on how erosion modified aerodynamic roughness length causes different saltation intensity, but this is already done in the recent paper by Webb et al. (2020). We have therefore not included the discussion on aerodynamic roughness in our paper.

*Manuscript structure*

*I think the manuscript mixes unnecessarily theory with results. I think the theory (Eqs. 4, 5, 6 etc. and related text) should be moved to the Methods section. In that Methods section I think it would be worthwhile explaining carefully how the parameter values of the modelling were chosen (rationale and assumptions) so that it is clear to the reader how the results have been produced. I find it strange not to have a Discussion section. I wonder if much of the detail in the Introduction would be better moved to the Discussion and then extended as necessary with additional context for the discussion. This would also help the Introduction quickly move the reader through the main issue.*

We have now substantially reworked on the manuscript. We hope that the views of Referee 3 are properly reflected in the revised paper.

## Reply to Dr. Sylvain Dupont

We are most grateful to Dr. Sylvain Dupont for carefully reading our manuscript and providing insightful and detailed comments for discussion. These comments are very valuable for improving our paper.

Dr. Dupont first commented on the results of the Khalfallah et al. (2020) paper and pointed out possible discrepancies between his own analysis and the results presented in Khalfallah et al. Indeed, our paper is triggered by the study of Khalfallah et al. which helped us decide to finally have a thorough look at the PSD issue. We thought this issue was resolved until the questions raised by the Kok paper which has caused a stir in the dust research community. Now, our results show the PSD at dust emission is  $u_*$  dependent. This seems also to be the view of Dr. Dupont. With respect to PSD dependency on atmospheric boundary-layer stability, our results seem to support the finding of Khalfallah et al. qualitatively, but we have some considerations of their interpretation why this might be so. We are not convinced that “diffusion” caused this dependency.

As we do not know exactly, how colleagues Khalfallah et al. processed their data, we cannot judge the reliability of their conclusion. Dr. Dupont is in a much better position to make the judgement, as he works with the authors of the afore-mentioned paper. With the insight Dr. Dupont provided, we modified in the revised paper and to be more cautious with the interpretation of the results of Khalfallah et al., although we have certainly tried not to “rely” on their work.

The second point of Dr. Dupont is important, namely, that he is convinced of PSD dependency on  $u_*$ , not necessary on ABL stability. Our view is somewhat different. In our paper, we have tried to make it clear that there is a mean  $u_*$  and a  $u_*$  variance, the PSD of dust at emission is not only dependent on the  $u_*$  mean but also on the  $u_*$  variance. This dependency arises because the saltation bombardment is non-linearly dependent on  $u_*$ . In essence, this is the problem of saltation/dust emission intermittency. In a series of related studies (e.g. Klose et al. 2014), we have been considering how turbulence causes dust emission. Suppose the mean  $u_*$  is  $u_{*i}$ , then there would be no saltation and no saltation bombardment, but if  $u_*$  has a distribution, then intermittent saltation and saltation bombardment will occur, and the PSD of dust at emission will be dependent on the PDF of  $u_*$ . This really is the main point of this study, and the idea is already in several Klose et al. papers.

Now, does turbulence intensity (actually the PDF of  $u_*$ ) depends on ABL stability? We think so, as the large-eddy simulation of Klose et al. (2014) shows and also the JADE observations. We have carried out recently a wind-tunnel experiment, again showing the dependency of  $u_*$  PDF on ABL stability and the strong impact on dust emission. The results of the wind-tunnel experiments will be summarized and sent for consideration of publication in our next paper on the subject.

Thanks for mentioning the Kaimal and Finnigan (1994) book (Yaping Shao and John Finnigan have worked in the same group for some years and is one of the first readers of the book). The  $r_{uw}$  curve in Fig 1.9 of KJ (1994) book does not seem to apply here, because (1) there is nothing said about the variance of the shear stress only the mean; (2) it only states that shear stress normalized with the wind variances is fairly constant (not exactly constant, actually why not exactly?); (3) earlier measurement of shear stress was mainly down somewhere in the ABL at some level, not really close enough to the surface; and (4) their Fig 1.10 actually shows that the variance of wind is dependent on ABL stability (i.e. the variance normalized with  $w_*$  is fairly universal).

We agree with Dr. Dupont, and we need to do more cases, as Ref. 2 also mentioned. In the revised paper, we used all JADE data and have done more case studies.



Dr. Dupont made several very helpful suggestions.

(1) more figures for characterizing the events: to understand what happened during the erosion events 10 and 11, show time variation of dust and saltation PSD during the events.

This is a good idea. We have done more data analysis.

(2) PSD of emitted dust flux.

We have added emission-flux PSD. In the revised text, we clarified the differences between the various definitions of PSDs.

(3) Condensation

As far as we know, there was no condensation, but there were a few drops of rainfall accompanied with the cool change, although no rainfall was recorded. We have looked into this and have addressed this problem in the revised manuscript.

(4) Enhanced cohesion in night.

This is an interesting point, but it is difficult to validate. However, we included Event-12 in the new study, which shows cohesion plays a big role in dust PSD.

In a separate study by the first author (unpublished), the modelling of soil moisture under extremely dry conditions is been worked out.

(5) Surface modified by saltation.

Yes. This is likely, but we cannot validate this.

(6) First justifications.

Dr. Dupont is right. We changed the manuscript.

(7)  $u_*$  variance.

This is an important point. As Dupont et al. (2018) shows that  $u^*$  needs to be averaged over 15 to 30 min for the flux-gradient relationship. However, there is no doubt that shear stress fluctuates due to large eddies, and shear stress has a pdf. This pdf is important to dust emission which rapidly responses to surface shear stress. The selection of 1min for shear stress averaging seems to be reasonable, this is to assume that saltation can reasonably respond to shear stress variations on this scale. This is the whole point of this paper. We are willing to debate with Dr Dupont on this in greater detail. In the revised manuscript, we added a discussion section addressing some of the issues related.

(8) Saltation bombardment intensity.

We have discussed this above. KF (1994) book, Fig. 1.9 states  $r_{uw}$  is almost independent of  $z/L$ , but  $r_{uw}$  is shear stress normalized with flow velocity variance which varies strongly with stability, as their Fig. 1.10 shows. But we agree with Dr. Dupont, this is an unsolved issue, because we do not fully understand how the laminar layer close to the surface behaves. There are theories about the possibility that the laminar layer breaks up. Our unpublished wind-tunnel experiment (measuring shear stress using Irwen sensors showing the fluctuations of shear stress related to large eddies). Again, the whole point is that we have to move away from the tradition “mean” flow approach and consider more the PDF of the turbulence quantities, which are important to understanding the PSD of dust at emission.

There seems to be a misunderstanding somewhere. What we try to say in justification 3 (now the second) is actually that the diffusion aspect due to enhanced or not enhanced turbulence with respect to instability does not affect the saltation trajectory too much. In this sense, Dr. Dupont is right. But the initial velocities of the saltation particles seem to be important.

It is great to discuss with colleague Dr. Dupont.

## Reply to Dr. Jasper Kok

We greatly appreciate Colleague Dr. J. Kok for his comments. That Dr. Kok took time to provide such thoughtful comments shows the need to clarify the dust PSD issue.

First, “Airborne-dust PSD” as “emission-dust PSD”: to our best knowledge, “emission-dust PSD” has never been directly observed. All emission-dust PSDs reported are airborne-dust PSDs or derived from airborne-dust PSDs. The various dust PSDs are sometimes confused in the literature. In the revised paper, we explicitly discussed this problem. The JADE airborne dust PSDs are of good quality and are probably close(r) to dust emission PSD.

The argument that dust advection depends on  $u_*$  is interesting, but does not seem to apply here. Advection is  $\sim u \partial C / \partial x \sim u_* \partial C / \partial x$ . In case of weak dust concentration gradient, advection does not play a major role. The JADE site is fairly homogeneous and the dust PSDs are measured close to the surface. Therefore, we can safely exclude the influence of advection on dust PSD.

Second, “Consistency of Evidence”. We have now checked this. The results presented in Shao et al. (2011) is based on 3.5m-OPC airborne-dust PSD for Event-10 and the results are correct. Colleague Dr. Kok and others have made excellent suggestions, so we have looked into the entire JADE dataset. Event-10 stands out as the only case, when dust PSD shows no clear  $u_*$  dependency. This is interesting. We have now pointed this out in the paper and have provided some interpretations.

Statistical significance test is generally lacking in dust related studies and this is partially why we have so much confusion in aeolian research. We have now showed a lot of data and added a discussion section dedicated to the uncertainties of the analysis.

Third, earlier results: We like this suggestion of Dr. Kok very much. But, to be honest, this is difficult, as it is hard to get to the bottom of the various data sets. We believe Dr. Kok and colleagues have properly estimated the error margins of the previously published data. However, based on Kok, 2011b Table S1, the data used seem to be airborne-dust PSD. Also, the data shown in Figure 4 of Mahowald et al. 2013 ([doi.org/10.1016/j.aeolia.2013.09.002](https://doi.org/10.1016/j.aeolia.2013.09.002)) are mostly airborne-dust observations (mixed with emission-flux PSDs). We have now show that airborne-dust PSDs have height dependency. A proper scaling of dust concentration profile will be necessary, before all these profiles can be compared.

Fourth, statistics: This is a very good suggestion. We added error margins and sample sizes in the graphs.

5th Line 30-32: “Since inter-particle cohesion depends on particle size,  $d$ , the fraction of dust emitted must also depend on  $d$ . Thus, for a given soil, the particle size distribution of dust at emission (emission-dust PSD),  $ps(d)$ , must depend on saltation bombardment or on friction velocity” and line 140-1 “ $u_*$  is a descriptor of saltation bombardment intensity”. This argument implicitly assumes that the impact speed of saltating particles increases with the friction velocity. It is highly intuitive that it would, but there is a very solid body of research that indicates that particle impact speed actually does not depend on friction velocity for transport-limited saltation. This lack of dependence of particle speed on wind speed was first proposed by Ungar and Haff (1987) because particle-wind feedbacks force an approximately constant saltator impact speed. It has since been confirmed by a large body of experimental (e.g., Namikas (2003), Rasmussen and Sorensen (2008), Creysells et al. (2009), Ho et al., (2011), Martin and Kok (2017)) and numerical (e.g., Duran et al. (2011), Kok et al. (2012)) work. The authors can of course present evidence to support their viewpoint counter to this literature, but I recommend acknowledging this extensive literature.

This is interesting. Let us make two thinking experiments. Exp 1:  $u^* = u^*_t$ , particle creeps and has impact velocity 0. Exp 2:  $u^* > u^*_t$ , particle saltates and has impact velocity larger than 0. This shows particle impact depends on  $u^*$ . But thanks for pointing out the study which conclude differently. Nevertheless, in very strong saltation and very weak surface binding, it is possible that dust PSD dependency on  $u^*$  is less obvious, as it seems to be case for Event-10.

6th Line 48-9: “Kok (2011a, 2011b) then proposed an emission-dust PSD and estimated its parameters from airborne-dust PSDs.” That’s actually not quite correct: Kok (2011a) only used emitted dust size distribution because airborne-dust PSDs are a convoluted sum of emission and advection (see comment above and by Sylvain Dupont). Also, the years on the references are incorrect (I corrected them in the quote above).

As far as we can see, Kok (2011a) used airborne-dust PSD.

7th I’m a bit confused how to interpret the 0-0.25 m/s  $u^*$  category in the present paper’s Figure 3, as this would include events without saltation where dust is not actively emitted but only advected. I suspect the authors are only using data for which saltation was occurring. If so, I recommend that the authors note that. And if not, I recommend the authors subset the data to only include active saltation data.

Saltation is intermittent and occurs below 0.25 m/s  $u^*$ . This is a point we try to make, namely, turbulence (and saltation intermittency) plays an important role in dust PSD. It seems that this point did not come across clearly, as this also appears to be the impression of colleague Dr. Dupont. However, we have followed the suggestion of Dr. Kok and have tested to average dust PSDs conditioned with  $Q > 0.1 \text{ gm}^{-1}\text{s}^{-1}$ , but the results are almost the same.

Many thanks to Colleague Dr. J. Kok.

### **List of Changes Made to the Manuscript:**

- (1) Substantial rework on the JADE data. We now use the whole JADE dataset for the analysis
- (2) Added Event-10, Event-11 and Event-12 as case study
- (3) Redone most of the graphs
- (4) Added a section for discussion
- (5) Clarified a number of issues raised by the referees, Dr. Dupont and Dr. Kok
- (6) Clarified the definitions of emission-dust PSD, airborne-dust PSD and emission-flux PSD
- (7) Pointed out the dependency of airborne-dust PSD on height
- (8) Pointed out that emission-flux PSD representing the dependency of dust concentration gradient on particle size
- (9) Added error-bars and sample size in graphs deemed to be useful
- (10) Numerous minor improvements

Please refer to the marked version for modification details.

# 1 **Dependency of Particle Size Distribution at Dust Emission on** 2 **Friction Velocity and Atmospheric Boundary-Layer Stability**

3 Yaping Shao<sup>1</sup>, Jie Zhang<sup>2</sup>, Masahide Ishizuka<sup>3</sup>, Masao Mikami<sup>4</sup>, John Leys<sup>5,6</sup>, Ning Huang<sup>2</sup>

4 <sup>1</sup>Institute for Geophysics and Meteorology, University of Cologne, Germany

5 <sup>2</sup>Key Laboratory of Mechanics on Disaster and Environment in Western China, Lanzhou University, China

6 <sup>3</sup>Faculty of Engineering and Design, Kagawa University, Japan

7 <sup>4</sup>Office of Climate and Environmental Research Promotion, Japan Meteorological Business Support Center, Japan

8 <sup>5</sup>[Office/Department of Planning, Industry and Environment and Heritage](#), New South Wales, Australia

9 <sup>6</sup>[The Fenner School of Environment & Society, The Australian National University, Australia](#)

10

11 *Correspondence to:* Jie Zhang [✉\(zhang-j@lzu.edu.cn\)](mailto:zhang-j@lzu.edu.cn) and Ning Huang [✉\(huangn@lzu.edu.cn\)](mailto:huangn@lzu.edu.cn)

12 **Abstract.** Particle size distribution of dust at emission (dust PSD) is an essential quantity to be estimated in dust studies. It  
13 has been recognized in earlier research that dust PSD is dependent on soil properties (e.g. whether soil is sand or clay) and  
14 friction velocity,  $u_*$ , a surrogate for surface shear stress and descriptor for saltation bombardment intensity. This recognition  
15 has been challenged in some recent papers, causing a debate on whether dust PSD is “invariant” and the search for [its](#)  
16 justification. In this paper, we ~~analyze~~[analyze](#) dust PSD measured in the Japan-Australian Dust Experiment and show that  
17 dust PSD is dependent on  $u_*$  and on atmospheric boundary-layer ([ABL](#)) stability. By simple theoretical and numerical  
18 analysis, we explain the ~~three~~[two](#) reasons for the latter dependency-, [both related to enhanced saltation bombardment in](#)  
19 [convective turbulent flows](#). First, ~~under similar mean wind conditions, the mean of  $u_*$  is larger for unstable than for stable~~  
20 ~~conditions.~~ [Second](#),  $u_*$  is stochastic and its probability distribution profoundly influences the magnitude of the mean saltation  
21 flux due to the non-linear relationship between saltation flux and  $u_*$ . ~~Third~~[Second](#), in unstable conditions, turbulence is  
22 usually stronger, which leads to higher saltation-bombardment intensity. This study confirms that dust PSD depends on  $u_*$ ,  
23 and more precisely, on the probability distribution of  $u_*$ , which ~~itself is stability dependent.~~ [We restate that for a given soil,](#)  
24 [finer dust is released in case of stronger saltation in turn is dependent on ABL stability, and consequently dust PSD is also](#)  
25 [dependent on ABL. We also show that the dependency of dust PSD on  \$u\_\*\$  and ABL stability is made complicated by soil](#)  
26 [surface conditions. In general, our analysis reinforces the basic conceptual understanding that dust PSD depends on saltation](#)  
27 [bombardment and inter-particle cohesion.](#)

28

## 29 1 Introduction

30 Gillette (1981) explained that dust emission can be produced by aerodynamic lift and saltation bombardment, but under  
31 realistic wind, aerodynamic-lift emission is much weaker than saltation-bombardment emission. This hypothesis was  
32 confirmed by Shao et al. (1993). It is recognized that saltation bombardment is the most important mechanism for dust  
33 emission, and dust emission rate,  $F$ , is proportional to streamwise saltation flux,  $Q$ <sup>1</sup>.

34 Rice et al. (1995, 1996) visualized the process of saltation bombardment using wind-tunnel photos: a saltation particle at  
35 impact on surface ejects a tiny amount of soil into air, leaving behind a crater. Models for estimating crater size have been  
36 developed by, e.g., Lu and Shao (1999). The fraction of dust that gets emitted from the ejection is difficult to estimate,  
37 because it depends both on inter-particle cohesion and bombardment intensity. Since inter-particle cohesion depends on  
38 particle size,  $d$ , the fraction of dust emitted must also depend on  $d$ . Thus, for a given soil, the particle size distribution of dust  
39 at emission (emission-dust PSD),  $p_s(d)$ , must depend on saltation bombardment or on friction velocity,  $u_*$  ( $\sqrt{\tau}/\rho$  with  $\tau$  being  
40 surface shear stress and  $\rho$  air density); see Section 4.2 for discussion). Alfaro et al. (1997) confirmed that  $p_s(d)$  depends on  
41  $u_*$ : as  $u_*$  increases,  $p_s(d)$  shows a higher fraction of dust of smaller  $d$ . Based on this result and the observations that different  
42 laboratory techniques for PSD analysis yield profoundly different outcomes, depending on the disturbances applied to the  
43 samples (Figure 1), Shao (2001) suggested to use a minimally-disturbed PSD,  $p_m(d)$ , as the limit of  $p_s(d)$  for weak saltation,  
44 and a fully-disturbed PSD,  $p_f(d)$ , as the limit of  $p_s(d)$  for strong saltation. In this way,  $p_s(d)$  is approximated as a weighted  
45 average of  $p_m(d)$  and  $p_f(d)$ , namely,

$$46 \quad p_s(d) = \gamma p_m(d) + (1 - \gamma) p_f(d) \quad (1)$$

47 where  $0 \leq \gamma \leq 1$  is an empirical function of  $u_{*f}(d)$ , the threshold friction velocity for particles of size  $d$ .

48 What is emission-dust PSD? We must distinguish three closely related yet subtly different dust PSD, namely, emission-  
49 dust PSD, airborne-dust PSD, and emission-flux PSD. PSD of dust in air (airborne-dust PSD) has been collected from  
50 different places under different conditions. ~~Airborne dust PSD and emission dust PSD are not the same, unless airborne dust~~  
51 ~~is observed close to the dust source and the dependency of particle diffusivity on  $d$  is neglected.~~ Emission-dust PSD and  
52 airborne-dust PSD are identical, if the latter is measured at dust source at height zero. Airborne-dust PSD can be used to  
53 approximate emission-dust PSD if it is measured close to the source and the dependency of particle motion in air on particle  
54 size can be neglected. For modelling size-resolved dust concentration in air (i.e. solving the dust concentration equation for  
55 different particle sizes), emission-dust PSD offers the Dirichlet-type boundary condition. If size-resolved dust-emission-  
56 fluxes can be calculated, then we can specify the Neumann-type boundary condition for solving the dust concentration  
57 equation. From size-resolved dust-emission-fluxes, an emission-flux PSD can be calculated (Section 2; Section 4.2).  
58 Emission-flux PSD is neither emission-dust nor airborne-dust PSD, but describes how vertical dust-concentration gradient

---

<sup>1</sup>The ratio  $\gamma_b = F/Q$  is a main issue of dust emission studies (Zender et al., 2003; Laurent et al., 2006). Marticorena et al. (1997) showed that  $\gamma_b$  depends on soil clay content. Shao (2004) suggested that  $\gamma_b$  depends on friction velocity, soil type and soil particle size distribution.

59 [depends on particle size. In some earlier publications, unfortunately, the differences between the three dust PSDs are not](#)  
60 [clearly explained.](#)

61 [To our knowledge, emission-dust PSD has never been directly measured, but approximated using airborne-dust PSD](#)  
62 [measured at some, often different, heights \(e.g. Kok, 2011b, Table S1\).](#) Available data of airborne-dust PSDs give the  
63 impression that they do not differ much. It has thus been suggested that airborne-dust PSDs may be “not-so-different” and  
64 hence emission-dust PSDs may also be “not-so-different”. Reid et al. (2008) stated that “on regional scales, common mode  
65 dust is not functionally impacted by production wind speed, but rather influenced by soil properties such as  
66 geomorphology ...”. Kok (~~2001a, 2001b~~2011a, 2011b) proposed a dust emission model by treating dust emission as a  
67 process of aggregate fragmentation by saltation bombardment. Since aggregate fragmentation is similar to brittle  
68 fragmentation, the size distribution produced in the process is scale-invariant (Astrom, 2006). Kok (~~2001a, 2001b~~2011a,  
69 2011b) then proposed an emission-dust PSD and estimated its parameters from ~~airborne dust PSDs~~the data listed in Table  
70 S1 of Kok (2011b). The proposed emission-dust PSD is frequently used in dust models (Giorgi et al., 2012; Albani et al.,  
71 2014; Pisso et al., 2019). However, whether the “not-so-different” airborne-dust PSDs justify “brittle fragmentation” as the  
72 underlying process for dust emission requires scrutiny.

73 ~~In comparison,~~[Studies on dust PSD are yet to deliver definitive answers.](#) The airborne-dust PSD measurements of  
74 Rosenberg et al. (2014) pointed to larger fraction of fine particles than in earlier published data. ~~Khalfallah et al. (2020)~~  
75 ~~reported that airborne dust~~[Ishizuka et al. \(2008\) found that airborne-dust PSD measured close to surface depends on  \$u\_\*\$  for a](#)  
76 [weakly crusted soil. Sow et al. \(2009\) examined the dependency of emission-flux PSD on  \$u\_\*\$  for three dust events and](#)  
77 [reported that the PSD appeared to be independent on  \$u\_\*\$ , but differed significantly between weak and strong events. In line](#)  
78 [with Sow et al. \(2009\), Khalfallah et al. \(2020\) reported that emission-flux PSD depends on atmospheric boundary-layer](#)  
79 (ABL) stability, and attributed this to the dependency of particle diffusivity on particle size. They stated that the dependency  
80 of emission-dust PSD on  $u_*$ , as observed by Alfaro et al. (1997), may be of secondary importance in natural conditions  
81 compared to its dependency on ABL stability.

82 [The argument of Khalfallah et al. \(2020\) rests on the preferential particle diffusion in turbulent flows. Csanady \(1963\)](#)  
83 [suggested that particle eddy diffusivity,  \$K\_p\$ , is related to eddy diffusivity,  \$K\$ , by](#)

$$K_p = K(1 + \beta^2 w_t^2 / \sigma^2)^{-1/2} \quad (2)$$

84  
85  
86  
87 [where  \$\beta\$  is a coefficient,  \$w\_t\$  particle terminal velocity and  \$\sigma\$  the standard deviation of \(vertical\) turbulent velocity. The](#)  
88 [analyses of Walklate \(1987\) and Wang and Stock \(1993\), among many others, reached similar conclusions. For dust particles](#)  
89 [smaller than  \$10\mu\text{m}\$ ,  \$K\_p/K\$  is close to one for  \$\sigma = 0.5\text{ms}^{-1}\$ , and still larger than 0.95 for  \$\sigma = 0.1\text{ms}^{-1}\$  \(Shao, 2008; Fig. 8.12\).](#)  
90 [Thus, preferential particle diffusion does not seem to fully explain the dependency of dust PSD on ABL stability.](#)

91 The confusion surrounding emission-dust PSD prompted us to re-examine the data of Ishizuka et al. (2008) from the  
92 Japan-Australian Dust Experiment (JADE). In JADE, airborne-dust PSD were measured at small height directly above the



93 dust source and can be assumed to well ~~represents approximate~~ the emission-dust PSD. ~~Hence, hereafter we no longer~~  
 94 ~~distinguish airborne and emission dust PSD but simply refer emission dust PSD as dust PSD.~~ By composite analysis for  
 95 different  $u_*$  and ABL stabilities, we show that dust PSD depends on  $u_*$ , supporting the findings of Alfaro et al. (1997), and  
 96 depends on ABL stability, supporting consistent with the findings of Khalfallah et al. (2020). But in contrast to Khalfallah et  
 97 al. (2020), we argue that these dependencies are not mutually exclusive, but collectively point to the simple physics that  
 98 emission-dust PSD is dependent on saltation-bombardment intensity and efficiency.

## 99 **2 JADAJADE Data**

100 JADE was carried out during 23 Feb ~ 14 Mar 2006 on an Australian farm at (33°50'42.4"S, 142°44'9.0"E) (Ishizuka et al.,  
 101 2008, 2014). The 4 km<sup>2</sup> farmland was flat and homogeneous such that the JADE data are not affected by fetch. In JADE,  
 102 atmospheric variables, land surface properties, soil PSD ~~and~~, size-resolved sand fluxes and dust fluxes-concentrations were  
 103 measured. Size-resolved dust-emission fluxes were estimated from the dust concentration measurements. Three Sand  
 104 Particle Counters (SPCs) (Mikami et al., 2005) were used to measure the sand fluxes in the size range of 39 - 654  $\mu\text{m}$  in 32  
 105 bins at 0.05, 0.1 and 0.3 m above ground at a sampling rate of 1 Hz. Using the sand fluxes,  $q_j$  ( $j = 1, 32$ ), the PSD of saltation  
 106 particles (saltation-flux PSD) is estimated for a particle size bin at  $d_j$  with bin size  $\Delta d_j$  as

$$107 \quad p(d_j)\Delta d_j = q_j / \sum_{j=1}^{j=32} q_j \quad (2)$$

108 Dust concentration was measured using Optical Particle Counters (OPC) for 8 size groups: 0.3 – 0.6, 0.6 – 0.9, 0.9 – 1.4,  
 109 1.4 – 2.0, 2.0 – 3.5, 3.5 – 5.9, 5.9 – 8.4 and  ~~$\gt; 8.4 - 12.0 \mu\text{m}$~~  at 1, 2 and 3.5m above ground. ~~The data for the  $\gt; 8.4 \mu\text{m}$  bin~~  
 110 ~~were excluded from analysis, as the~~ The upper size limit was for the last bin is not well defined, but set empirically to  
 111 12.0  $\mu\text{m}$  such that this bin can still be included in the analysis. Airborne-dust PSD is estimated as

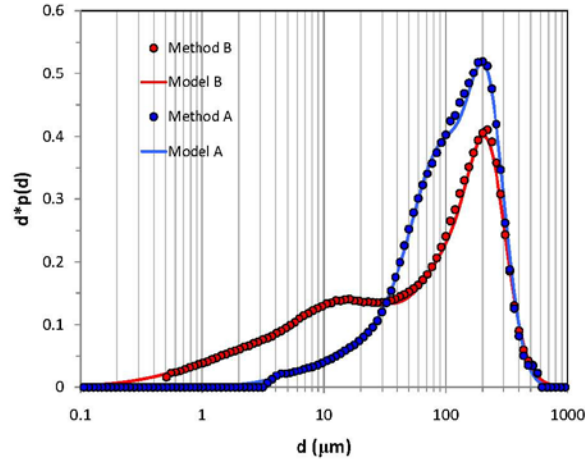
$$112 \quad p(d_j)\Delta d_j = c_j / \sum_{j=1}^{j=7} c_j \quad (3)$$

113 where  $c_j$  denotes the dust concentration for size bin  $j$ . Similarly, the emission-flux PSD can be defined as

$$114 \quad p(d_j)\Delta d_j = F_j / \sum F_j \quad (3a)$$

115 where  $F_j$  denotes the dust flux for size bin  $j$ . It should be noted that the emission-flux PSD describes how the covariance of  
 116 particle-velocity and particle-concentration depends on particle size, not the concentration itself. In this study, we use the  
 117 airborne-dust PSD observed at 1m to approximate emission-dust PSD, and use the airborne-dust PSD observed at 3.5m and  
 118 the emission-flux PSD derived from the 3.5m- and 1m-OPC measurements for additional discussions (Section 4.2).  
 119 Hereafter, emission-dust PSD approximated using the 1m-OPC airborne-dust PSD is simply referred to as dust PSD, unless  
 120 otherwise explicitly stated.

121 Atmospheric variables, including wind speed, air temperature and humidity at various levels, radiation and precipitation  
 122 were measured using an automatic weather station. These quantities were sampled at 5-second intervals and their 1-minute  
 123 averages were recorded- (see Section 4.2 for discussions). Two anemometers mounted at 0.53 and 2.16m measured wind  
 124 speed. From the atmospheric data, the Obukhov length,  $L$ , sensible heat flux,  $H$ , and friction velocity,  $u_*$ , were derived.<sup>2</sup> Also  
 125 measured were soil temperature and moisture.



126  
 127 Figure 1. Soil particle-size distribution obtained using Method A and Method B, together with the respective approximations (Model A  
 128 and Model B).

129 Surface soil samples were taken and soil PSD was analysed in laboratory using Method A and B with a particle size  
 130 ~~analyzer~~analyser (Microtrac MT3300EX, Nikkiso). In Method A, water was used for sample dispersion with no ultrasonic  
 131 action. In Method B, sodium hexametaphosphate (HMP) 0.2% solution was used for sample dispersion and 1-minute  
 132 ultrasonic action of 40W was applied. Following the convention of sedimentology, the soil is ~~loamy sand based Method A,~~  
 133 ~~and~~ sandy loam based on the analysis using Method B. Figure 1 shows  $p_A(d)$  (soil PSD from Method A) and  $p_B(d)$  (soil PSD  
 134 from Method B) and the corresponding approximations:  $p_A$  shows a larger fraction of particles in the range of 30~300 $\mu\text{m}$ ,  
 135 while  $p_B$  a larger fraction of particles in the range of 0.1~30 $\mu\text{m}$ .

136 An overview of the JADE data is shown in Figure 2. During ~~JADE~~the experiment, 12 significant aeolian events were  
 137 recorded, as marked in the figure. Most of the events occurred under unstable ABL conditions. Several quantities can be  
 138 used as a measure of ABL stability, but the one used here is the convective scaling velocity,  $w_*$ , defined as

139

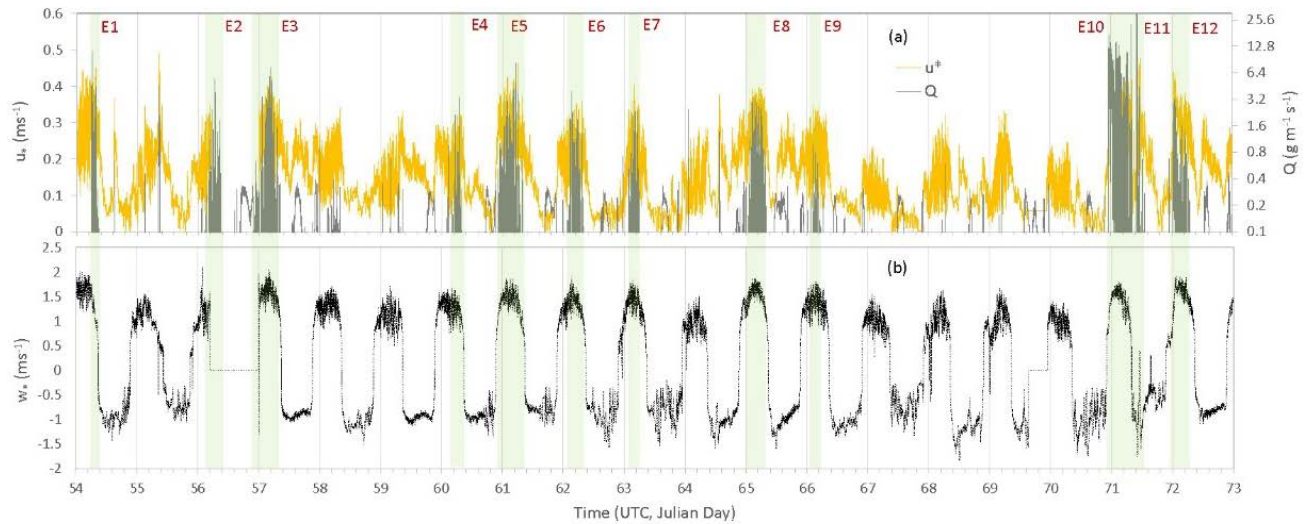
$$w_* = \left( \frac{g}{\theta} H_0 z_l \right)^{\frac{1}{3}} \tag{4}$$

<sup>2</sup> Drag-partition theory (Raupach, 1992; Webb et al., 2020) tells that shear stress,  $\tau = \rho u_*^2$ , is not the same as the shear stress,  $\tau_s$ , experienced by soil particles, due to roughness sheltering. For JADE, the surface is bare and thus the effect of roughness sheltering is neglected. The saltation fluxes used in this study are measured and do not involve the assumption  $\tau = \tau_s$  or otherwise.

140 where  $g/\bar{\theta}$  is the buoyancy parameter with  $g$  being the acceleration due to gravity and  $\bar{\theta}$  the mean potential temperature;  $H_0$  is  
141 surface kinematic heat flux ( $\text{Kms}^{-1}$ ) and  $z_i$  a scaling length (set to the capping inversion height for convective ABL and 100m  
142 for stable ABL). For unstable conditions,  $w_*$  is positive while for stable conditions  $w_*$  is negative. The reason for choosing  $w_*$   
143 is that it is a scaling parameter for the strength of turbulence. Usually,  $w_*$  is not used for stable ABLs, but is used here as an  
144 indicator for the suppression of turbulence by negative buoyancy.

145 In addition to the 12 events, a number of weak and intermittent events occurred. In this study, we first use the whole  
146 dataset for dust PSD analysis, and then use the data for Event-10, 11 and 12 for case studies. These three events are chosen  
147 for that Event-10 is the strongest event during JADE, Event-11 is one that occurred at night under stable conditions, while  
148 Event-12 occurred with a weakly crusted soil surface (Ishizuka et al., 2008).

149



150

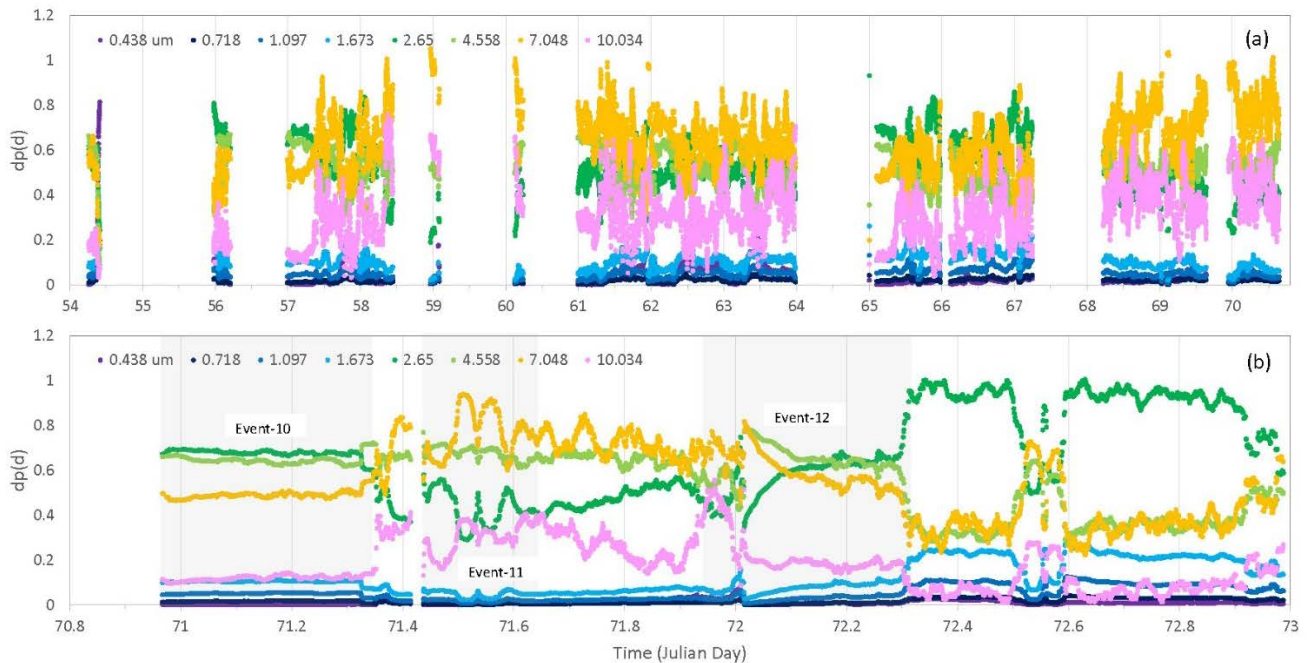
151 Figure 2. (a) One-minute averaged friction velocity,  $u_*$ , and streamwise saltation flux,  $Q$ , for the JADE observation time period; (b) One-  
152 minute averaged convective scaling velocity,  $w_*$ . In addition to the 12 aeolian events marked, a number of weaker and intermittent aeolian  
153 events occurred.

154

### 3 Results

155

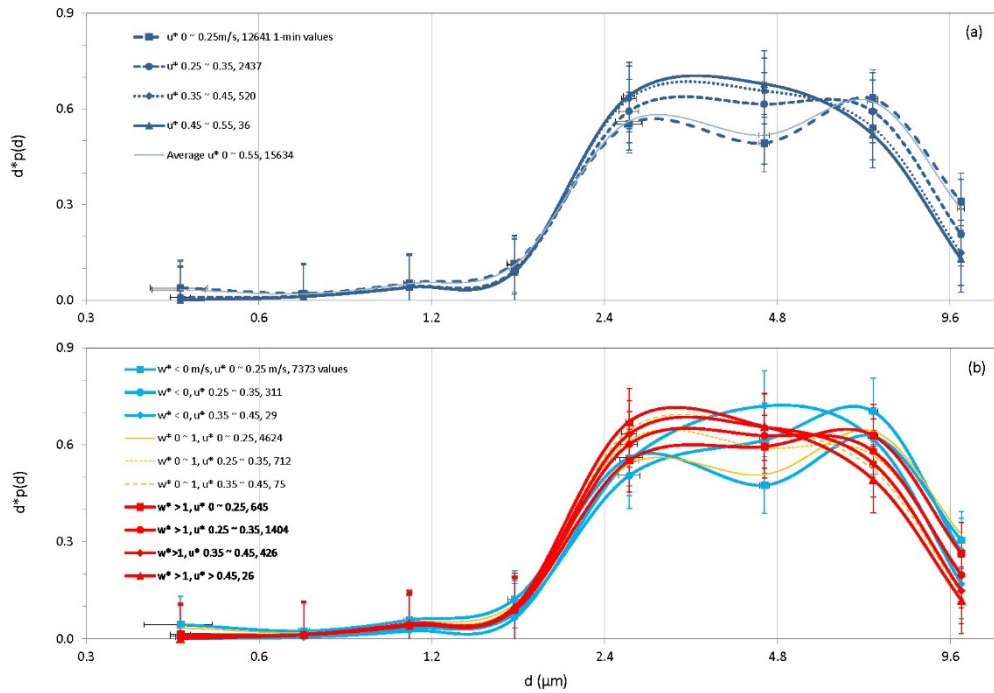
#### 3.1 Overall Results



156

157 [Figure 3. Dust PSD measured at 1m using OPC for the entire JADE observation period plotted in two sections, \(a\) for section Julian day](#)  
 158 [54 ~ 70.8 and \(b\) for section Julian day 70.8 ~ 73.0.](#)

159 [Plotted in Figure 3 are the time series of dust PSD for the entire JADE period, which show rich temporal variations,](#)  
 160 [probably apart from Event-10. To examine dust-PSD dependency on friction velocity, we use  \$u\_\*\$  to denote the one-minute](#)  
 161 [values of friction velocity,  \$p\(u\_\*\)\$  its probability density function \(PDF\),  \$\bar{u}\_\*\$  its mean and  \$\sigma\_{u\_\*}\$  its standard deviation. The  \$u\_\*\$](#)   
 162 [values are divided into the categories of 0~0.25, 0.25~0.35, 0.35~0.45 and 0.45~0.55  \$\text{ms}^{-1}\$ , and the corresponding dust PSDs](#)  
 163 [and saltation PSDs are sorted accordingly. These  \$u\_\*\$  categories correspond roughly to intermittent, weak, moderate and](#)  
 164 [strong saltation, respectively. The threshold friction velocity,  \$u\_{\*t}\$  for the JADE site is around  \$0.2\text{ms}^{-1}\$ , but intermittent](#)  
 165 [saltation has been observed oft at  \$u\_\*\$  below this  \$u\_{\*t}\$ . The dust PSDs are then composite averaged for the  \$u\_\*\$  categories. Figure](#)  
 166 [4a shows the dust PSDs for the different  \$u\_\*\$  categories and the mean dust PSD, i.e., dust PSD averaged over all  \$u\_\*\$  categories](#)  
 167 [\(including a total of 15634 one-minute points\). We ~~select~~ have repeated the same averaging procedure using a subset of the](#)  
 168 [JADE data, conditioned with  \$Q > 0.1\text{gm}^{-1}\text{s}^{-1}\$  and found that the results are very similar to those presented in Figure 4. The](#)  
 169 [mean dust PSD shows an interesting local minimal at  \$\sim 4\mu\text{m}\$ . This is attributed to the lack of particles of this size in the  \$u\_\* <\$](#)   
 170 [0.25 \$\text{ms}^{-1}\$  category. Figure 4a shows that dust PSD clearly depends on  \$u\_\*\$ , particularly in the size range 2~10 \$\mu\text{m}\$ . In general, as](#)  
 171  [\$u\_\*\$  increases, the fraction of fine dust particles increases. For the submicron size range, the dependency of dust PSD on  \$u\_\*\$  is](#)  
 172 [less definitive. The dust PSD for the  \$u\_\* < 0.25 \text{ms}^{-1}\$  category shows a higher fraction of submicron dust particles, especially](#)  
 173 [in stable conditions \(Figure 4b\). Apart from this, the results shown in Figure 4a are consistent with the findings of Alfaro et](#)  
 174 [al. \(1997\) that dust PSD is  \$u\_\*\$  dependent.](#)



175

176 [Figure 4. \(a\) Dust PSD for different  \$u\_\*\$  categories derived from the whole JADE dataset; \(b\) as \(a\), but for the different  \$u\_\*\$](#)   
 177 [categories under stable \( \$w\_\* < 0\$ \), moderately unstable \( \$0 < w\_\* < 1 \text{ ms}^{-1}\$ \) and unstable \( \$w\_\* > 1 \text{ ms}^{-1}\$ \) conditions.](#)

178

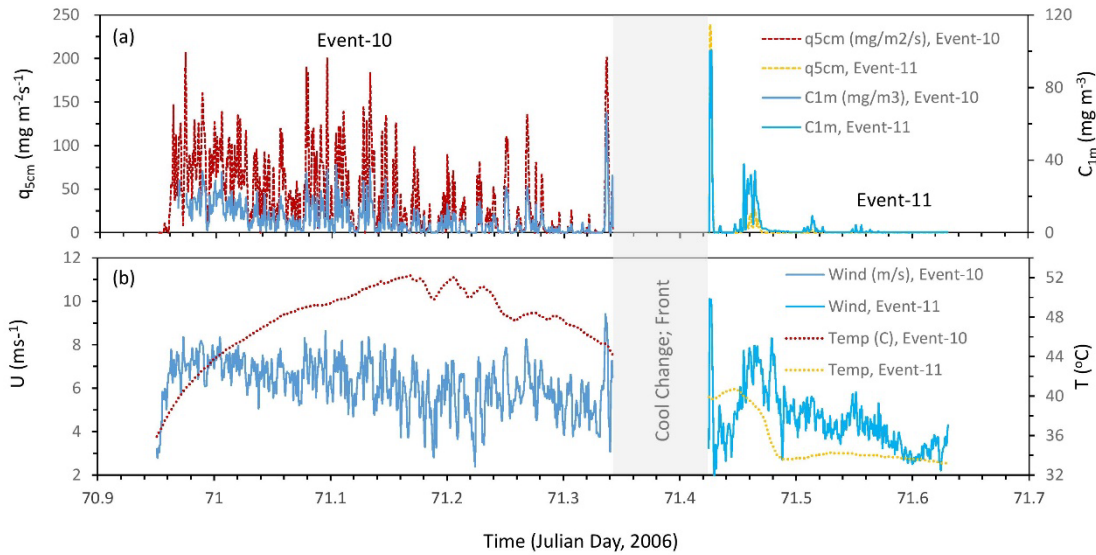
179 [To examine the dust PSD dependency on ABL stability, we divide the dataset into three, namely, stable \( \$w\_\* < 0\$ \),](#)  
 180 [moderately unstable \( \$0 < w\_\* < 1 \text{ ms}^{-1}\$ \) and unstable \( \$w\_\* \geq 1 \text{ ms}^{-1}\$ \) stability classes. For each stability class, the dust PSD data](#)  
 181 [are regrouped according to the  \$u\_\*\$  categories. Figure 4b shows the dust PSDs averaged for different  \$u\_\*\$  categories and stability](#)  
 182 [classes. For given stability class, dust PSD shows dependency on  \$u\_\*\$ , and for a given  \$u\_\*\$  category, dust PSD shows](#)  
 183 [dependency on  \$w\_\*\$ . For given  \$u\_\*\$ , the mode of dust PSD shifts systematically to finer particles as the ABL becomes more](#)  
 184 [unstable.](#)

185

### 186 [3.2 Case Study Results](#)

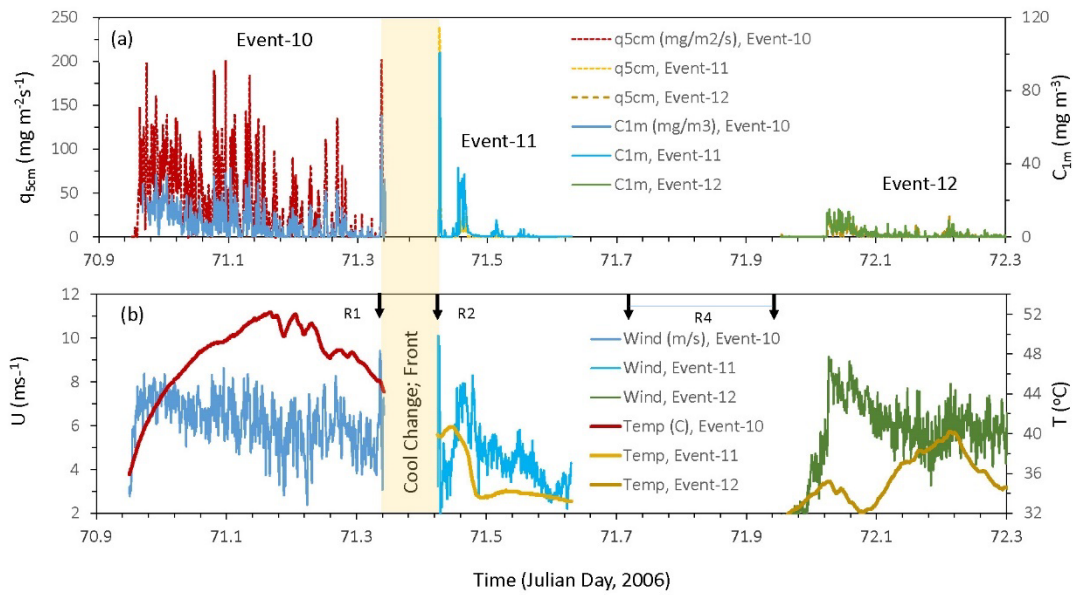
187 [We now study the cases of Event-10 \(09:49~19:13 12 Mar 2006; Julian Day 70.9506940~71.3423611\) and, Event-11](#)  
 188 [\(21:12 12 Mar ~ 02:08 13 Mar 2006, Julian Day 71.4250000~71.6305600\) for the analysis, because Event 10 occurred](#)  
 189 [under daytime unstable, while Event 11 under night time stable, conditions. Figure 263056\) and Event-12 \(09:54~18:58 13](#)  
 190 [Mar 2006, Julian Day 71.95417~72.33194\). Figure 5 shows the one-minute averages of wind speed at 0.53m,  \$U\$ , air](#)  
 191 [temperature at 0.66m,  \$T\$ , saltation flux at 0.05m,  \$q\_{\text{sem}}\$ , and total dust concentration \(summed over all particle size bins\) at 1m,](#)  
 192  [\$C\_{1\text{m}}\$ . Event-10 occurred ~~on~~ under daytime unstable conditions. It was a very hot day prior to a cool change \(cold front causing](#)  
 193 [temperature drop but no rainfall\), with near surface air temperature reaching  \$52^\circ\text{C}\$  and wind speed  \$\sim 8 \text{ ms}^{-1}\$ . ~~Event 10~~The](#)

194 [event](#) lasted ~10 hours. The cool change occurred at ~19:00-21:00 13 Mar 2006 local time. [While precipitation was not](#)  
 195 [recorded by the rain gauge \(with resolution of 0.2 mm\), the rain sensor \[PPS-01\(C-PD1\), PREDE Co. Ltd.\], as marked in](#)  
 196 [Figure 5b, sensed an event of raindrops shortly before the cool change, lasting about two minutes, and shortly after, lasting](#)  
 197 [about one minute \(Ishizuka et al., 2008\).](#) The strong winds (probably also strong sand drift and dust emission) accompanying  
 198 the cool change caused the shutdown of the instruments and thus, unfortunately, this period was not fully recorded. Event-11  
 199 occurred [under stable conditions](#) after the cool change in the ~~nighttime~~ [night time](#) of 12/13 Mar 2006, during which  $T$  was  
 200 dropping from  $\sim 40^{\circ}\text{C}$  to  $\sim 33^{\circ}\text{C}$  and  $U$  from  $\sim 8\text{ms}^{-1}$  to  $\sim 5\text{ms}^{-1}$ . Event-11, [which can also arguably be considered to be](#)  
 201 [part of Event-10,](#) was much weaker than Event-10.



202  
 203 [As the OPC measurements were taken close to the surface and directly above the dust source, the dust-concentration](#)  
 204 [values were generally high. For Event-10, the mean, standard deviation, maximum and minimum of  \$C\_{1\text{m}}\$  are respectively](#)  
 205 [7.56, 8.56, 65.96 and 0.02  \$\text{mg m}^{-3}\$ , and for Event-11 3.05, 10.57, 100.17 and 0.04  \$\text{mg m}^{-3}\$ . The extremely high dust](#)  
 206 [concentrations measured shortly before and after the cool change could be affected by dust advection and are excluded from](#)  
 207 [the analysis \(although their inclusion made no difference to the event averages of the dust PSDs\). For other times, it can be](#)  
 208 [safely assumed that the dust observed was locally emitted.](#)

209



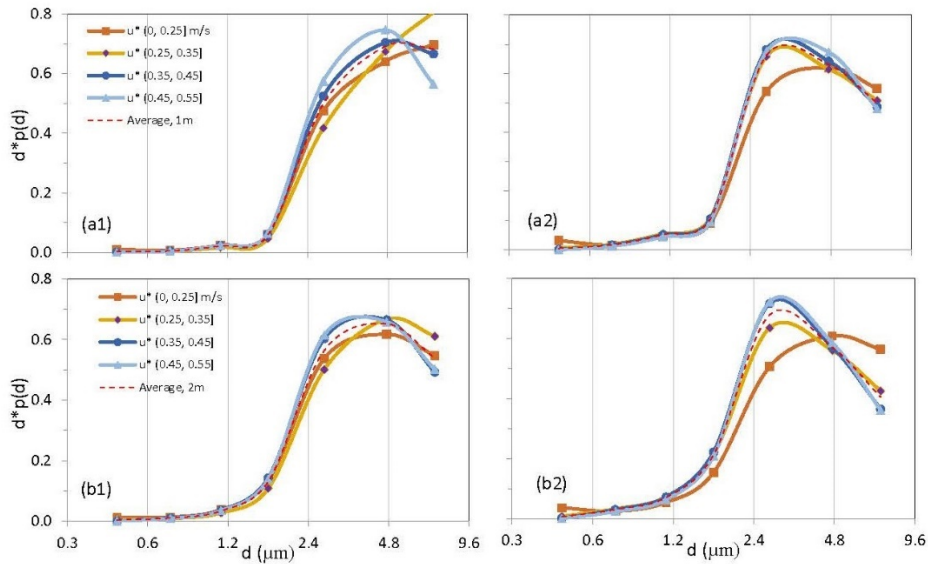
210

211 Figure 25. (a) one-minute averaged saltation flux at 0.05m,  $q_{5cm}$ , and dust concentration at 1m,  $C_{1m}$ , for Event-10, -11 and  
 212 Event-11-12; (b) as (a) but for wind speed at 0.53m above ground,  $U$ , and air temperature at 0.66m,  $T$ . The cool change is  
 213 marked and the three rain events sensed by the rain sensor are marked as R1, R2 and R4 using the black arrows.

214

### 3-Results

215 ~~To examine dust PSD dependency on friction velocity, we use  $u_{*z}$  to denote the one minute values of friction velocity,  $p(u_{*z})$  its~~  
 216 ~~probability density function (PDF),  $\bar{u}_{*z}$  its mean and  $\sigma_{u_{*z}}$  its standard deviation. The  $u_{*z}$  values are divided into the categories of~~  
 217 ~~0-0.25, 0.25-0.35, 0.35-0.45 and 0.45-0.55  $ms^{-1}$ , and the corresponding dust PSDs and saltation PSDs are sorted accordingly.~~  
 218 ~~These PSDs are then composite averaged for the  $u_{*z}$  categories. As Figure 3 shows that for both Event 10 and -11, at both 1m~~  
 219 ~~and 2m height, as  $u_{*z}$  increases, the mode of dust PSD shifts to finer particles. For Event 10, the most obvious shift occurs~~  
 220 ~~between the  $u_{*z}$  categories 0-0.25 $ms^{-1}$  and 0.25-0.35  $ms^{-1}$ , while the shift between the 0.35-0.45  $ms^{-1}$  and 0.45-0.55  $ms^{-1}$  is~~  
 221 ~~less pronounced. The results shown in Figure 3 are consistent with the findings of Alfaro et al. (1997) and show that dust~~  
 222 ~~PSD is  $u_{*z}$ -dependent.~~

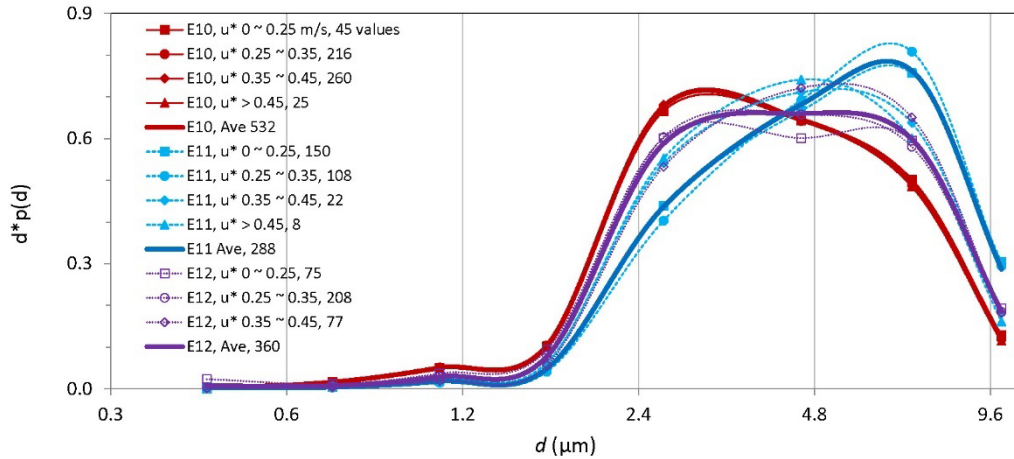


223

224 [Figure 3](#)

225 [Event-12 is developed shortly after the weak rainfall event \(R4\). Again, while precipitation was not recorded by the rain](#)  
 226 [gauge \(i.e. total rainfall was less than 0.2 mm\), the rain sensor reported rain drops during 71.70625~71.95278. Ishizuka et al.](#)  
 227 [\(2008\) reported that Event-12 is unique for JADE, because it is the only case when the soil surface was weakly crusted. We](#)  
 228 [will show later how dust PSD can substantially evolve even within one dust event, as soil surface conditions change \(Figure](#)  
 229 [10\).](#)

230



231

232 [Figure 6. Dust PSD for different  \$u\_\*\$  categories for Event-11 at levels 1m and 2m \(a1 and b1\), and for Event-10 \(a2 and b2\), 10, 11 and](#)  
 233 [12. Also shown are the PSDs averaged over all  \$u\_\*\$  values \(red dashed line\) categories for the individual events.](#)



234 Figure 3 shows also that the dust PSDs for Event-10 and -11 considerably differ. As said, Event-10 occurred under  
235 unstable, while Event-11 under stable conditions. Several quantities can be used as measure of ABL stability, but the one  
236 used in this study is the convective scaling velocity defined as

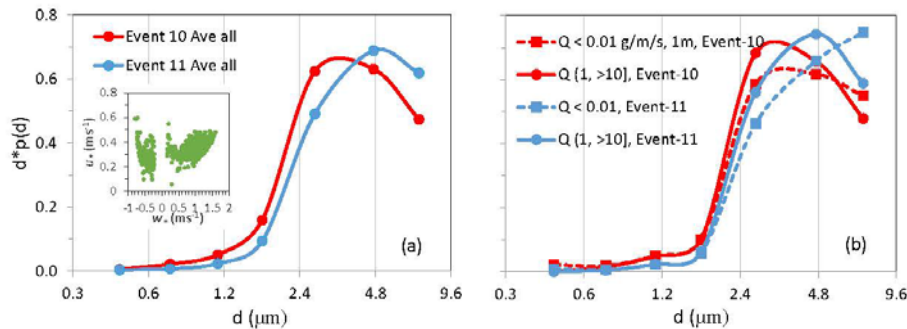
$$237 \quad w_* = \left( \frac{g}{\bar{\theta}} H_0 z_l \right)^{\frac{1}{3}} \quad (4)$$

238 ~~where  $g/\bar{\theta}$  is the buoyancy parameter with  $g$  being the acceleration due to gravity and  $\bar{\theta}$  the mean potential temperature;  $H_0$  is~~  
239 ~~surface kinematic heat flux ( $\text{Kms}^{-1}$ ) and  $z_l$  a scaling length (set to the capping inversion height for convective ABL and 100m for~~  
240 ~~stable ABL). For unstable conditions,  $w_*$  is positive while for stable conditions negative. The reason for choosing  $w_*$  is that it is a~~  
241 ~~scaling parameter for the strength of turbulence in unstable ABL. Usually,  $w_*$  is not used for stable ABLs, but used here as~~  
242 ~~an indicator for the suppression of turbulence by negative buoyancy.~~

243 Figure 4a shows the dust PSD averaged over three (1, 2 and 3.5m) heights and all  
244  $u_*$  values for Event-10 and -11. The insert shows a scatter plot of  $u_*$  against  $w_*$  for  
245 Event-10 (right half) and -11 (left half). Figure 6 shows the dust PSDs for the different  $u_*$  categories  
246 for Event-10, 11 and 12. For Event-11 and 12, the dependency of dust PSD on  $u_*$  is obvious, in agreement with the overall  
247 results shown in Figure 4a. The dust PSD for Event-10 shows no clear dependency on  $u_*$ , an observation also reported in  
248 Shao et al. (2011). Our basic argument for dust PSD dependency on  $u_*$  rests upon the assumption that saltation-impact speed  
249 is  $u_*$  dependent. It has been suggested that impact-particle speed may not strongly depend on  $u_*$  for transport-limited  
250 saltation (Ungar and Haff, 1987), because particle-flow feedbacks force an approximately constant saltation-impact speed.  
251 While this argument is supported by some experimental evidence (Martin and Kok, 2017) and numerical simulations (Duran  
252 et al., 2012; Kok et al., 2012), its general validity and the conditions for its validity need further examination. JADE Event-  
253 10 is probably a case which comes closest to meet the requirements of strong particle-flow feedback and sustained  
254 equilibrium of saltation for the Ungar and Haff (1987) hypothesis to apply. In addition, Event-10 occurred on an extremely  
255 hot and dry day, with the 0.66m air temperature reaching  $\sim 52^\circ\text{C}$  and the 0.66m relative humidity dropped below 3%. It is  
256 likely that under such extreme weather conditions, the inter-particle cohesion is destroyed. These factors combined may be  
257 responsible for the lack of dust PSD dependency on  $u_*$  for Event-10 (Figure 6). But for all other JADE events, the  
258 dependency of dust PSD on  $u_*$  is significant.

259 The event-averaged dust PSDs for Event-10, -11 and -12 clearly differ. For Event-10, the mean and standard deviation of  
260  $u_*$  and  $w_*$  were respectively (0.36, 0.057) and (1.03, 0.29), all in  $\text{ms}^{-1}$ , and for Event-11 (0.28, 0.077) and (-0.41, 0.159).  
261 From Event-10 to -11, the dust PSD mode shifted from about  $3\mu\text{m}$  to  $56\mu\text{m}$ . During Event-10, a substantially higher fraction  
262 of particles in the size range of  $0.4 \sim 4\mu\text{m}$  ~~was emitted~~exists. To further examine how dust PSD depends on saltation  
263 intensity, we ~~average~~have averaged the dust PSDs for different  $Q$  categories. ~~Examples of the dust PSDs for  $Q < 0.01 \text{ gm}^{-1} \text{ s}^{-1}$~~   
264 ~~(weak saltation) and  $Q (1, >10) \text{ gm}^{-1} \text{ s}^{-1}$  (moderate to strong saltation) are (not shown in Figure 4b. Again).~~ It is found that  
265 weak saltation corresponded to coarser dust particles and strong saltation to finer dust particles, ~~i.e., in Event-10 finer~~

266 particles are emitted than in Event-11, a result that can also be seen in Figure 3. However, the composite analysis of dust  
 267 PSDs for the different  $Q$  categories shows that the dust PSD dependency on  $w_*$  persisted (Figure 4b). The results shown in  
 268 Figure 4a and 4b are6 confirm the dependency of dust PSD on ABL stability, consistent with those of Khalfallah et al.  
 269 (2020)-the overall results shown in Figure 4.



270  
 271 Figure 4. (a) Dust PSD averaged over all  $u_*$  values and over Event-10 and Event-11. The insert shows that the three levels 1, 2 and 3.5m wind conditions for  
 272 Event-10 and Event-11 were not too different, but Event-12 was much weaker. Figure 6 shows that also the  
 273 dust PSDs for the two events considerably differ, with Event-10 being the one with richer finer dust particles. Event-12 will  
 274 be further discussed in Section 4.2.

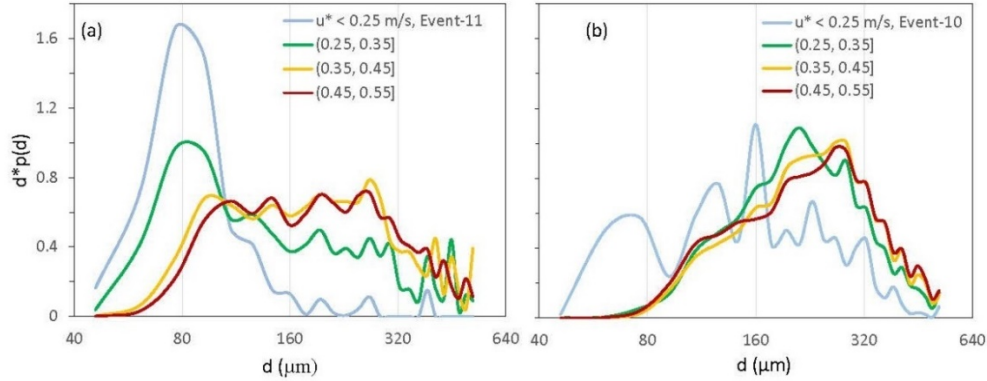
275 We make the following observations based on the JADE data: (1) Dust PSD has rich temporal variations and is a scatter  
 276 plot of  $u_*$  against  $w_*$  (not “universal”); (2) Dust PSDs averaged for the PSD depends on  $u_*$  and ABL stability; and (3) Dust  
 277 PSD is influenced by soil surface conditions. These observations support the conceptual understanding that dust PSD is  
 278 determined both by saltation flux categories  $Q < 0.01 \text{ gm}^{-1}\text{s}^{-1}$  and  $Q \{1, > 10\} \text{ gm}^{-1}\text{s}^{-1}$  for Event-10 bombardment and Event-11, by soil  
 279 binding strength (Shao, 2001, 2004).

## 280 4 Discussions

### 281 4.1 Influence of Turbulence on dust PSD

282 The reason for the dependency of dust PSD on  $u_*$  has been explained in Gillette et al. (1974), Gillette (1981), Shao et al.  
 283 (1993), Alfaro et al. (1997) and Shao (2001), because  $u_*$  is a descriptor of saltation bombardment intensity. In the earlier  
 284 explanations, only mean friction velocity and mean saltation are considered, while the turbulent nature of saltation  
 285 bombardment is implicitly neglected. But how is the dependency of dust PSD on ABL stability, here  $w_*$ , explained?  
 286 Khalfallah et al. (2020) attributed this to the different diffusion of particles of different sizes. The most conspicuous reason is  
 287 the enhanced saltation bombardment by turbulence in stable and unstable conditions. This interpretation does not seem to  
 288 apply to the JADE data, since the dust PSDs at 1, 2 and 3.5m levels do not substantially differ, and the dust particles

289 considered here are in a small size range (0.38–8.3 $\mu\text{m}$ ) such that their diffusivities should be all almost identical to the eddy  
 290 diffusivity.



291

292 Figure 57. (a) Saltation PSD averaged for four different  $u_*$  categories for Event-11; (b) as (a), but for Event-10.

293 ~~The most conspicuous reason~~ It is ~~the enhanced saltation bombardment in unstable conditions. Several observations can be~~  
 294 ~~made from~~ interesting to examine how dust PSD is related to saltation PSD. The saltation PSD for Event-10 and -11 are  
 295 shown in Figure 57. First, for  $u_* \leq 0.25\text{ms}^{-1}$  in Event-11, saltation PSD was confined to a narrow size range ~~centered~~  
 296 at 70~80 $\mu\text{m}$  where  $u_{*r}$  is minimum. This indicates that saltation splash/bombardment was weak to mobilize particles in other  
 297 size ranges. In contrast, for  $u_* \leq 0.25\text{ms}^{-1}$  in Event-10, saltation PSD covered a broader size range, implying that saltation  
 298 splash was strong to entrain particles of other sizes. Second, for both Event-10 and -11, the peak values of saltation PSD  
 299 were shifted to larger particles for larger  $u_*$ : for Event-10 the peak for  $u_* = 0.35\text{ms}^{-1}$  was at 203.3 $\mu\text{m}$ , while for  $u_* = 0.55\text{ms}^{-1}$   
 300 at 257.8 $\mu\text{m}$ . Clearly, since  $u_{*r}$  is particle size dependent, saltation PSD is a selective sample of the soil PSD by wind. Third,  
 301 the saltation PSDs for given  $u_*$  categories (e.g.,  $0.35 < u_* \leq 0.45\text{ms}^{-1}$ , Figure 5a8a and 5b8b) differed significantly between  
 302 Event-10 and -11 as a consequence of ABL stability. In Event-11 (Figure 5a8a), saltation was not fully developed, as the  
 303 saltation PSD plateau in the size range 100~300 $\mu\text{m}$  suggests, implying again that saltation splash/bombardment was not  
 304 efficient. In Event-10 (Figure 5b7b), saltation was more fully developed.

305 ~~Based on Figures 3, 4 and 5, we conclude that dust PSD~~The stronger saltation of Event-10 is ~~not only  $u_*$  but also  $w_x$~~   
 306 ~~dependent. We argue that the dependency on  $w_x$  can be~~partially attributed to ~~saltation bombardment intensity from three~~  
 307 ~~perspectives. First, the stronger wind and instability, which result in a larger  $\bar{u}_*$ , than in Event-11. It is known from the ABL~~  
 308 similarity theory that,

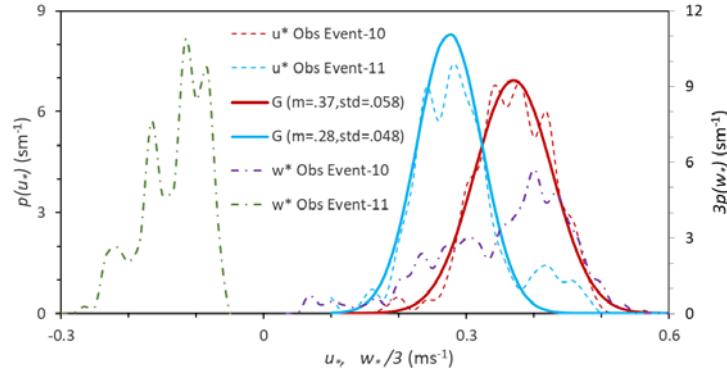
309 
$$\bar{u}_* = \frac{\kappa z}{\phi_m} \frac{\partial \bar{u}}{\partial z} \quad (5)$$

310 where  $\kappa$  is the von Karman constant,  $z$  height and  $\phi_m$  a similarity function (Stull, 1988):

311

$$\phi_m = \begin{cases} 1 + \beta_m \zeta & \zeta > 0 \text{ stable} \\ (1 - \gamma_m \zeta)^{-1/4} & \zeta < 0 \text{ unstable} \\ 1 & \zeta = 0 \text{ neutral} \end{cases} \quad (6)$$

312 where  $\zeta = z/L$  ( $L$  is Obukhov length) and  $\beta_m = 5$  and  $\gamma_m = 16$  are empirical coefficients (Businger et al., 1971). For stable  
 313 conditions,  $\phi_m > 1$  and for unstable conditions  $\phi_m < 1$ . Figure 68 shows the PDFs of  $u_*$  and  $w_*$  for Event-10 and -11,  
 314 together with the approximations for the PDFs of  $u_*$ . For Event-10,  $\bar{u}_* = 0.37\text{ms}^{-1}$ , while for Event-11,  $\bar{u}_* = 0.28\text{ms}^{-1}$ . ~~The~~  
 315 ~~larger  $\bar{u}_*$  was partly responsible for the stronger saltation and dust emission during Event 10 than during Event 11.~~



316

317 Figure 68. The probability density functions of  $u_*$  and  $w_*$ ,  $p(u_*)$  and  $p(w_*)$ , respectively, for Event-10 and -11, together with the Gaussian  
 318 approximations for the  $p(u_*)$  functions. The mean values (m) and standard deviations (std) for the Gaussian (G) distributions are given.  
 319 Note that for  $p(w_*)$ ,  $3p(w_*)$  against  $w_*/3$  is plotted to conveniently present the information in the same graph.

320 ~~Second, as Figure 6~~ We suggest that the dependency of dust PSD on  $w_*$  for given  $u_*$  is attributed to saltation bombardment  
 321 intensity from two perspectives. First, as Figure 8 shows,  $u_*$  is a stochastic variable. Li et al. (2020) suggested that  $\tau = \rho u_*^2$   
 322 neutral conditions is Gauss distributed. Klose et al. (2014) reported that  $\tau$  in unstable conditions is Weibull distributed. The  
 323 exact form of  $p(\tau)$  requires further investigation, but the JADE data of  $u_*$  show that  $p(u_*)$  is reasonably Gaussian. Hence,

324

$$p(\tau) = \frac{1}{2\rho u_*} p(u_*) \quad (7)$$

325 is skewed to smaller  $\tau$ . ~~Figure 6,~~ suggesting that the large-eddy model results of Klose et al. (2014) are qualitatively  
 326 reasonable. Figure 8 shows that  $u_*$  in Event-10 not only had a larger mean value but also a larger variance than in Event-11.  
 327 We emphasize that the variance of  $u_*$  strongly affects saltation, because saltation flux depends non-linearly on  $u_*$ . To  
 328 illustrate this, we consider  $u_{*1}$  and  $u_{*2}$ , and assume that

329

- $u_{*1}$  and  $u_{*2}$  are Gaussian distributed and have the same mean that equals  $u_{*i}$  (say  $0.2\text{ms}^{-1}$ )

330

- $u_{*1}$  and  $u_{*2}$  have respectively standard deviation,  $\sigma_1$  and  $\sigma_2$ , with  $\sigma_2 = \eta \sigma_1$  and  $\eta > 1$ ; and

331 •  $Q$  satisfies the Owen's model (Owen, 1964),

$$332 \quad Q_i = cu_{*i}^3 \left( 1 - \frac{u_{*t}^2}{u_{*i}^2} \right) \quad \text{for } u_* > u_{*t};$$

$$333 \quad \text{otherwise } 0; \quad \text{with } i = 1, 2 \quad (8)$$

334 where  $c$  is a dimensional constant. It follows that the ratio of the mean values of  $Q_2$  and  $Q_1$  is

$$335 \quad \eta_Q = \frac{\bar{Q}_2}{\bar{Q}_1} = \int_{u_{*t}}^{\infty} Q_2 p(u_{*2}) du_{*2} / \int_{u_{*t}}^{\infty} Q_1 p(u_{*1}) du_{*1} \quad (9)$$

336 Equation (9) can be evaluated numerically for different  $\eta$  (Table 1) and is approximately

$$337 \quad \eta_Q = 0.607 \eta^2 - 0.0028\eta + 0.4283 \quad (10)$$

338 This shows that  $p(u_*)$  profoundly influences the magnitude of  $Q$ . For fixed  $\bar{u}_*$ , a [larger](#)  $u_*$  variance corresponds to a  
339 larger  $\bar{Q}$ .

340 Table1. Streamwise saltation flux ratios,  $\eta_Q$ , for different  $u_*$  std ratios,  $\eta$  (see text for details).

$\eta$	1.2	1.4	1.6	1.8	2	3	4
$\eta_Q$	1.30	1.63	2.00	2.41	2.86	5.83	10.15

341 [ThirdSecond](#), in unstable conditions, turbulence is stronger due to buoyancy production, which leads to increased saltation  
342 bombardment intensity. We do not have independent evidence to verify this, but to illustrate the point, we use a two-  
343 dimensional (2-d,  $x_1$  in mean wind direction and  $x_3 \equiv z$  in vertical direction) saltation model (Supplement A) to simulate the  
344 impact kinetic energy of saltation sand grains. For given  $u_*$  and roughness length,  $z_0$ , a 2-d turbulent flow is generated with  
345 the mean wind assumed to be logarithmic  $\kappa \bar{u}_1 = \bar{u}_* \ln(z/z_0)$  and the velocity standard deviations satisfy  
346

$$347 \quad \frac{\sigma_{u1}}{\bar{u}_*} = a \cdot \ln \left( \frac{z}{z_0} \right) \quad (11)$$

$$348 \quad \frac{\sigma_{u3}}{\bar{u}_*} = f_{u3}(\zeta) \cdot a \cdot \ln \left( \frac{z}{z_0} \right) \quad (12)$$

349 and the dissipation rate for turbulent kinetic energy,  $\varepsilon$ , satisfies

$$350 \quad \varepsilon \frac{\kappa z}{\bar{u}_*^3} = f_\varepsilon(\zeta) \quad (13)$$

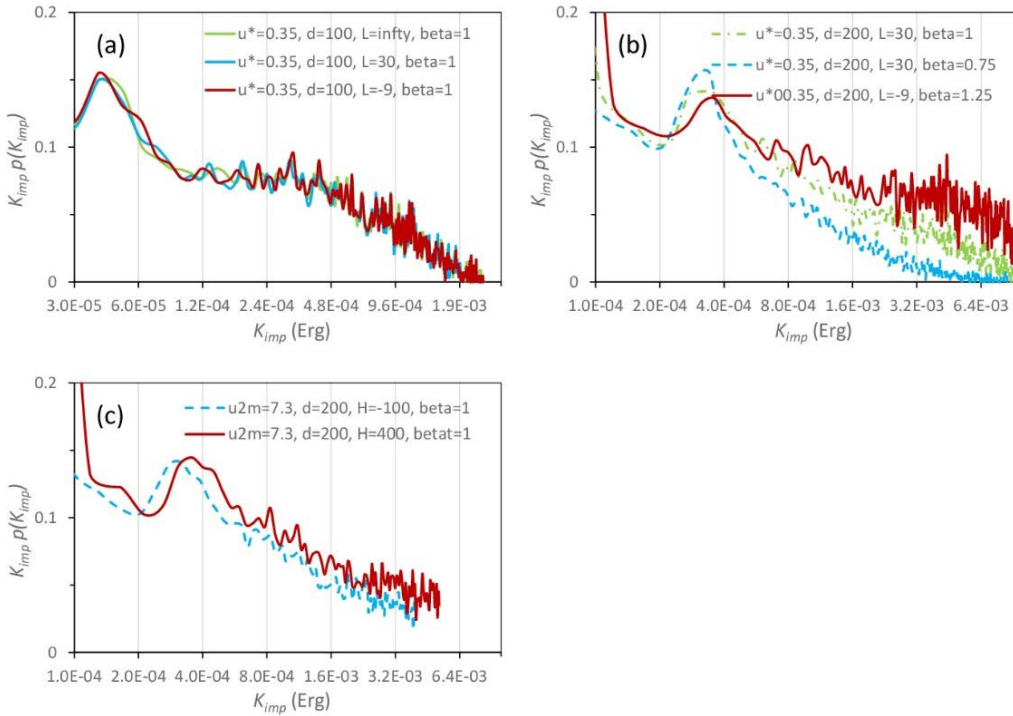
351 The similarity relationships  $f_{u3}(\zeta)$  and  $f_{\varepsilon}(\zeta)$  follow Kaimal and Finnigan (p16, 1995). As saltation takes place in the layer  
 352 close to the surface, the vertical profiles of  $\sigma_{u1}$  and  $\sigma_{u3}$  are considered following Yahaya et al. (2003). The coefficient  $a$   
 353 ( $=1.16\beta$ ) is varied by setting  $\beta$  to 0.75, 1.00 and 1.25 for weak, normal and strong turbulence, respectively.

354 In each numerical experiment, 20000 sand grains of identical size are released from the surface and their trajectories are  
 355 computed. At impact on the surface, the particles rebound with a probability of 0.95 and a rebounding kinetic energy,  $K_{reb}$ ,  
 356 0.5 times the impact kinetic energy,  $K_{imp}$ . The rebound angle is Gauss distributed with a mean of  $40^\circ$  and standard deviation  
 357  $5^\circ$ . Splash entrainment is neglected. The PDF of  $K_{imp}$ ,  $p(K_{imp})$ , is used as a measure for bombardment intensity.

358 Many numerical experiments ~~are~~ were carried out, but for our purpose, we show only the results of the ones listed in Table  
 359 2. The initial velocity components of sand grains ( $V_{1o}$ ,  $V_{3o}$ ) are generated stochastically.  $V_{1o}$  is Gauss distributed with a mean  
 360  $\bar{V}_{1o} = \bar{u}_* \cos(55^\circ)$  and standard deviation,  $\sigma_{V_{1o}} = 0.1\bar{u}_*$ .  $V_{3o}$  is Weibull distributed with a shape parameter  $A = 2$  and a scale  
 361 parameter  $B' = \bar{u}_* \sin(55^\circ) / \Gamma(1 + 1/A)$  where  $\Gamma$  is a Gamma function. To account for the influence of stability on  $V_{3o}$ ,  $B'$   
 362 is modified such that the adjustment to  $\sigma_{V_{3o}}$  is the same as that to  $\sigma_{u3}(10z_0)$ , i.e., the modified scale parameter,  $B$ , is given  
 363 by

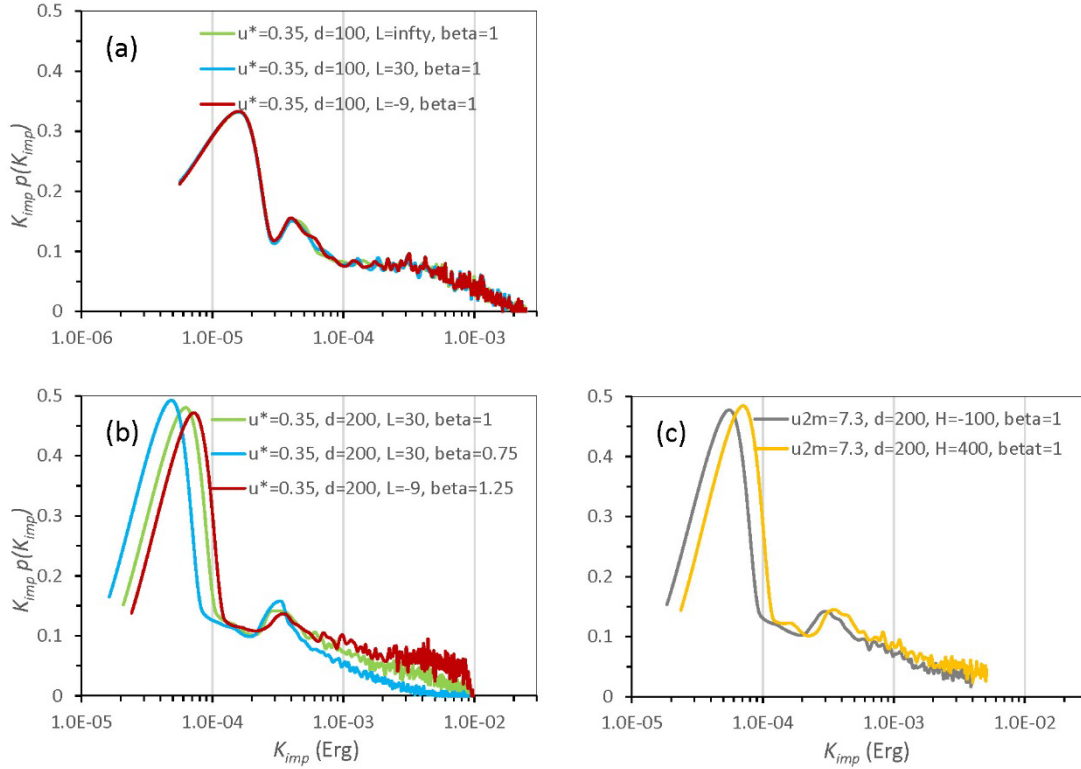
364

$$B = \beta f_{u3} \left( \frac{30z_0}{L} \right) \left( \frac{10z_0}{L} \right) B' \quad (14)$$



365

366



367

368 Figure 79. Probability density function  $p(K_{imp})$  (plotted in  $K_{imp}p(K_{imp})$  against  $K_{imp}$  in logarithmic scale) for the numerical experiments. In  
 369 (a),  $p(K_{imp})$  is shown for  $u_* = 0.35\text{ms}^{-1}$ ,  $d = 100\mu\text{m}$  and  $\beta = 1$  but for three different Obukhov lengths  $L = \infty$ , 30m and -9m. In (b), the effect  
 370 of  $\beta$  on  $p(K_{imp})$  is examined; and in (c) the effect of stability on  $p(K_{imp})$  with given mean wind speed at  $z = 2\text{m}$  is examined.

371 | Figure 7a9a compares  $p(K_{imp})$  for Exp1a, 1b and 1c and shows that  $p(K_{imp})$  for these cases is very similar. The small  
 372 differences in  $p(K_{imp})$  between the cases suggest that the differences in particle trajectory arising from the stability  
 373 modification to turbulence profile, with  $u_*$  fixed, are negligible. However, a small change in  $\beta$ , as Figure 7b9b shows for  
 374 Exp2a, 2b and 2c, can lead to significant changes in  $p(K_{imp})$  with larger  $\beta$  corresponding to higher probability of larger  $K_{imp}$ ,  
 375 namely, high saltation bombardment intensity. In Exp3a and 3b,  $u_{2m}$  (mean wind 2m height) is set to  $7.3\text{ms}^{-1}$  and the surface  
 376 sensible heat flux,  $H$ , to  $-100$  and  $400\text{Wm}^{-2}$ . Figure 7e9c shows that  $p(K_{imp})$  differs significantly with larger  $K_{imp}$  in unstable  
 377 conditions.

378 Table 2: Numerical experiments for saltation bombardment intensity. For all experiments,  $z_0 = 0.48\text{mm}$ ,  $C_0 = 5$ ,  $C_1 = 2$  and  $\rho_p = 2650\text{kgm}^{-3}$ .

Exp	$u_*$ ( $\text{ms}^{-1}$ )	$L$ (m)	$d$ ( $\mu\text{m}$ )	$\beta$
Exp1a, 1b, 1c	0.35	$\infty$ , 30, -9	100	1.0
Exp2a, 2b	0.35	30	200	0.75, 1
Exp2c	0.35	-9	200	1.25
Exp3a, 3b	$u_{2m} = 7.3$	$H = -100; 400\text{Wm}^{-2}$	200	1

379

380 ~~The experiments reveal that~~To summarize, the PDF of particle initial velocity influences strongly saltation bombardment  
381 ~~intensity, and saltation in in unstable ABL intensifies saltation bombardment to cause finer dust particle emission.~~

382 ~~The numerical experiments reveal suggest~~ that the PDF of the particle initial velocity influence significantly ~~on saltation~~  
383 ~~bombardment intensity, as influences~~ the saltation ~~bombardment intensity, and saltating~~ particles in unstable ABL impact the  
384 surface with larger kinetic energy than in stable ABL. This is ~~also~~ the result seen in Figure 58, i.e., saltation in Event-10 was  
385 more fully developed than in Event-11. The more fully developed saltation in unstable ABL increases saltation  
386 bombardment intensity and hence the release of finer dust particles, seen in Figure 46.

#### 387 **44.2 Influence of Surface Condition on Dust PSD**

388 A detailed analysis of Event-12 (Figure 10) reveals that the dependency of dust PSD on friction velocity and ABL stability  
389 is made complicated by soil surface conditions. To analysis how dust PSD evolved during the event, we divide Event-12 that  
390 lasted ~5.5 hours into 11 half hourly time sections labelled as S1, S2 etc. For each section the dust PSD is averaged over  
391 time and plotted in Figure 10c. Figure 10a shows the time series of  $Q$ ,  $w_*$  and  $u_*$ , and Figure 11b the time series of 2cm soil  
392 temperature and soil moisture. For the whole event, the ABL was unstable, with  $w_*$  fluctuating around  $1.64 \pm 0.12\text{ms}^{-1}$ .  
393 Initially (e.g. S1 and S2),  $u_*$  was relatively large, exceeding  $0.4\text{ms}^{-1}$  at times, but then eased to around  $0.3\text{ms}^{-1}$ .  $Q$  generally  
394 followed the variations of  $u_*$ . Yet, the dust PSD showed a systematic shift from coarser to finer particles, as the event  
395 progressed. The dust PSD dependency on  $u_*$  of Event-12 does not conform with the results for Event-11 (Figure 6) and the  
396 overall results (Figure 4a). Ishizuka et al. (2008) noticed that prior to Event-12, weak rainfall occurred (R4, Figure 5b) and  
397 consequently, weak crusts formed on the soil surface. Apparently, the lightly crusted surface prevented the emission of fine  
398 dust particles in the early stages of Event-12. As the event progressed, soil temperature increased, soil moisture decreased  
399 (Figure 10b) and the saltation during the early stages caused the destruction of the crusts and the amount of fine dust  
400 particles available for emission increased. These are the most likely reasons for why in the later stages of Event-12, an  
401 increased fraction of fine dust was released, although the atmospheric stability did not significantly change and  $u_*$  actually  
402 reduced.



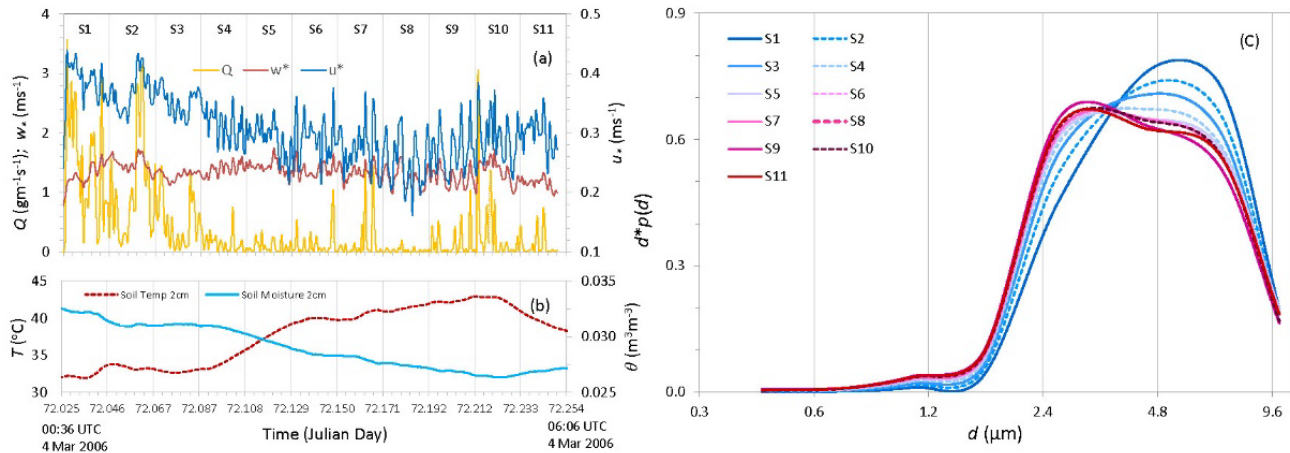
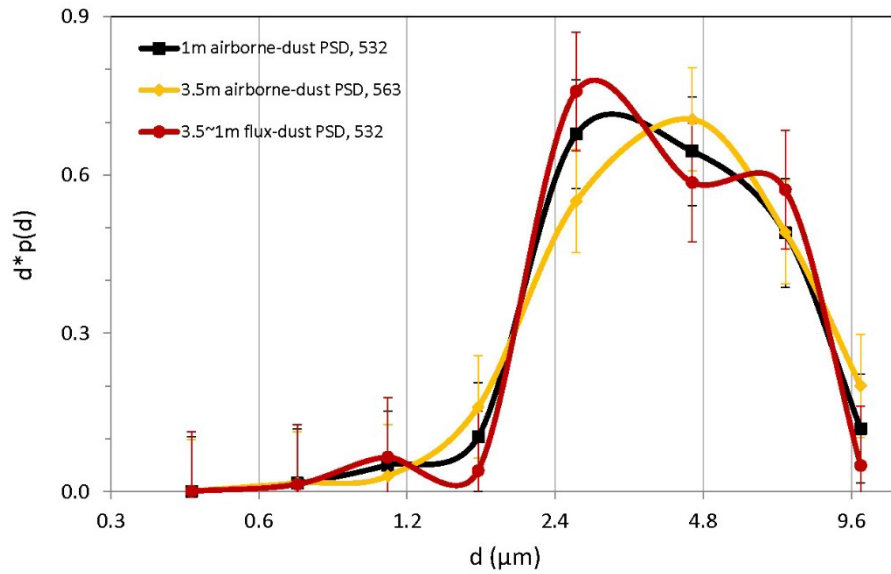


Figure 10. (a) Time series of streamwise saltation flux,  $Q$  ( $\text{gm}^{-1}\text{s}^{-1}$ ), convective scaling velocity,  $w_*$  ( $\text{ms}^{-1}$ ), and friction velocity,  $u_*$  ( $\text{ms}^{-1}$ ), for Event-12. The time span of Event-12 is divided into 11 half-hourly sections, labelled as S1, S2 etc. (b) As (a), but for soil temperature,  $T$  ( $^{\circ}\text{C}$ ), and soil moisture,  $\theta$  ( $\text{m}^3\text{m}^{-3}$ ), both at 0.02m depth. (c) Dust PSDs averaged over section S1, S2 etc.

### 4.3 Uncertainties

We now discuss several issues related to the uncertainties of the analysis. First, the approximation of emission-dust PSD with airborne-dust PSD measured at some height above ground causes uncertainties, because airborne-dust PSD is height dependent as consequence of the dust-transport processes (e.g. diffusion and deposition) in the atmosphere, which are both particle-size and turbulence-property dependent. As our understanding of these processes is not complete and dust measurements have inaccuracies, a careful selection of the data for the analysis is necessary. Figure 11 shows a comparison of Event-10 averaged airborne-dust PSDs at 1m and 3.5m. Ishizuka et al. (2014) suggested to exclude the 2m-OPC data, because they do not correlate well with the 1m- and 3.5m-OPC data. The PSDs derived from the 2m-OPC data do show unexpected differences in comparison to those from the 1m- and 3.5m-OPC data. We thus have excluded the 2m-OPC data from our analysis. The PSDs derived from the 1m- and 3.5m-OPC data somewhat differ, with the peak particle size shifted by about two microns, i.e., airborne-dust PSD has a noticeable change with height. This also implies that it would be very difficult to compare airborne-dust PSD measured at different locations and under different conditions without a well-established framework equivalent to the Monin-Obukhov similarity theory.

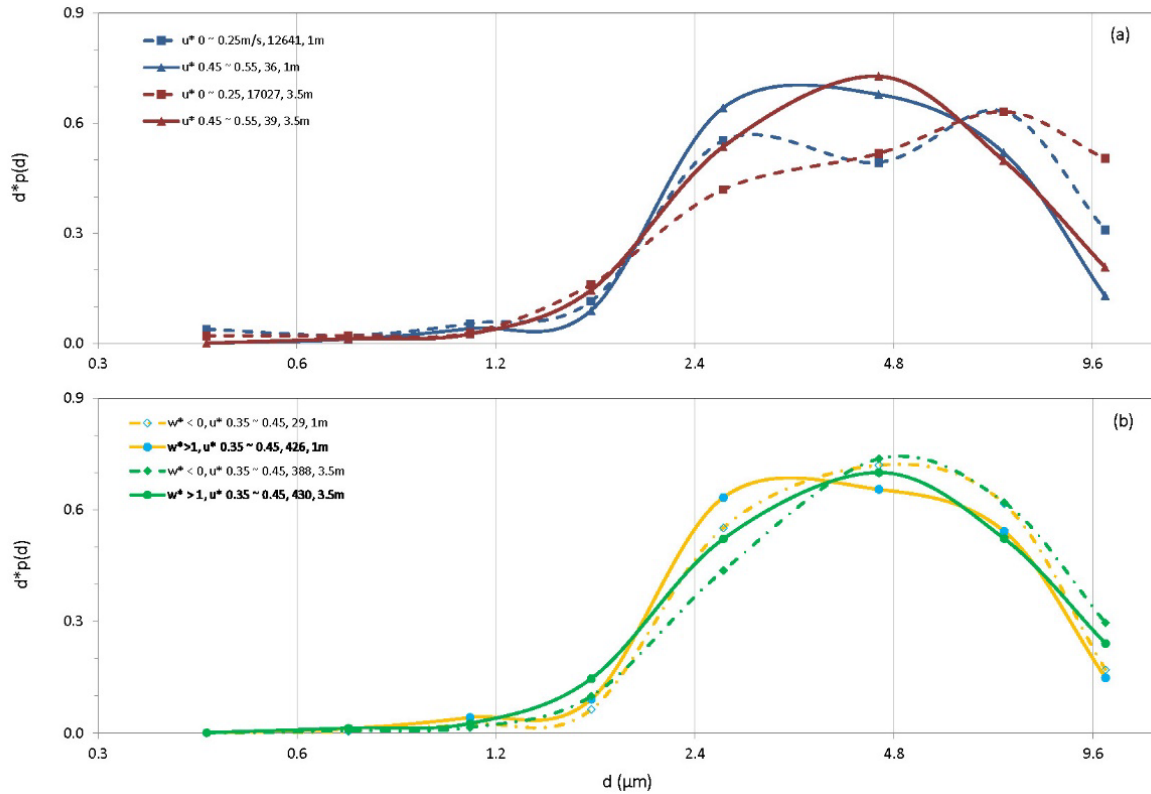
Also shown in Figure 11 is the Event-10 averaged emission-flux PSD calculated using Equation (3a). Dust fluxes for different particle size bins are calculated using the 3.5m- and 1m-OPC data with the gradient method (Gillette et al. 1972) and corrections (Shao et al. 2011). As dust flux is proportional to the negative gradient of dust concentration, emission-flux PSD basically describes how dust-concentration gradient [in our case  $-(c_{3.5\text{m}} - c_{1\text{m}})$ ] depends on particle size.



426

427 [Figure 11: JADE Event-10 averaged airborne-dust PSD measured at 1m \(532 one-minute samples\) and 3.5m \(563 one-](#)  
 428 [minute samples\) using OPCs. Also shown are standard-error bars. For comparison, Event-10 averaged \(over 532 one-minute](#)  
 429 [samples\) emission-flux PSDs calculated using Equation \(3a\) is plotted.](#)

430 [Although dust PSDs derived from 1m-OPC and 3.5m-OPC data differ, qualitatively they show similar dependencies of](#)  
 431 [dust PSD on  \$u\_{\*c}\$  and  \$w\_{\*c}\$ . Figure 12a compares the averaged dust PSDs for two  \$u\_{\*c}\$  categories using the 1m-OPC and 3.5m-OPC](#)  
 432 [data. For both cases, the dust PSD dependency on  \$u\_{\*c}\$  is visible. Figure 12b compares the averaged dust PSD for a given  \$u\_{\*c}\$](#)   
 433 [category \( \$0.35\sim 0.45\text{ms}^{-1}\$ \) under stable and unstable conditions. Again, both the 1m-OPC and 3.5m-OPC dust PSDs show](#)  
 434 [dependency on  \$w\_{\*c}\$ .](#)



435

436 [Figure 12: \(a\) JADE averaged airborne-dust PSD measured at 1 and 3.5m for two  \$u\_\*\$  categories. \(b\) As \(a\) but for one  \$u\_\*\$](#)   
 437 [category and two different stabilities.](#)

438

439 [It needs to be clarified whether using 1-minute averages of shear stress, saltation flux and dust flux are appropriate for the](#)  
 440 [study. Related to this question are two inter-wined yet somewhat different scaling issues, namely, \(1\) the scaling of turbulent](#)  
 441 [flux and the corresponding mean variable of boundary-layer turbulent flow \(i.e. the flux and gradient relationship\); and \(2\)](#)  
 442 [the scaling of aeolian fluxes and atmospheric forcing \(i.e. saltation/dust-emission intermittency\). It is usual in boundary-layer](#)  
 443 [meteorology to compute a turbulent flux from the profile of the corresponding mean quantity, e.g., mean shear stress from](#)  
 444 [mean wind profile, and the time interval for the mean is typically 15 to 30 minutes such that the assumptions of horizontal](#)  
 445 [homogeneity and stationarity commonly made in boundary-layer studies are met. This issue is not yet fully resolved even in](#)  
 446 [boundary-layer studies. For example, large-eddy models \(with spatial resolution of several meters and temporal resolution of](#)  
 447 [seconds\) frequently use the Monin-Obukhov similarity functions to estimate sub-grid surface stress from the grid-resolved](#)  
 448 [speed. In this study, we distinguish the 1-min averages of  \$u\_\*\$  from the mean shear stress of the boundary-layer flow to](#)  
 449 [emphasize the importance of shear stress fluctuations. The problem how to scale aeolian fluxes is not new \(e.g. Shao and](#)  
 450 [Mikami, 2005\). Dupont \(2020\) has a dedicated paper on this problem and stated that  \$u\_\*\$  is a suitable scaling parameter for](#)

451 dust flux over usual 15~30-min time intervals, but at smaller time resolution, wind becomes more relevant to scale dust  
452 fluxes, a conclusion similar to that reached in Sterk et al. (1998). The studies of Stout and Zobeck (1997) and Sterk et al.  
453 (1998), and more recently Klose and Shao (2012) and Klose et al. (2014), all pointed to the importance of taking  
454 instantaneous shear stress into consideration of aeolian dynamics. As Shao (2008, p203-205) explains,  $\tau_{inst} \sim U'^2$ , where  $\tau_{inst}$   
455 is instantaneous shear stress and  $U'$  instantaneous wind speed. The argument of Shao (2008) reasonably well explains the  
456 conclusions of Sterk et al. (1998) and Dupont (2020). Liu et al. (2018, Figure 7) analysed co-spectrum of saltation flux and  
457 shear stress and showed that they have a correlation peak at  $2 \times 10^{-3}$  Hz, corresponding to gusts/large eddies of around 10  
458 minutes in turbulent flows. These considerations suggest that to average shear stress and aeolian fluxes over one minute is  
459 appropriate and has the advantage of showing how dust emission is related to turbulence. We have emphasised throughout  
460 this paper that turbulence is key to understanding the dependency of dust PSD on ABL stability, because most essential  
461 difference among ABLs of different stability are the intensity and structure of turbulence.

462 As far as averaged dust PSDs are concerned, we have compared the dust PSDs averaged for different  $u_*$  categories using  
463 1-minute averaged data and 10-minute averaged data. The results are almost the same.

## 464 **5 Conclusions**

465 Using JADE data, we showed that dust PSD is dependent on friction velocity  $u_*$ . This finding is consistent with the wind-  
466 tunnel study of Alfaro et al. (1997). The JADE data support the claim that dust PSD is saltation-bombardment dependent and  
467 ~~does~~ not support the hypothesis that dust PSD is invariant.

468 The JADE data show that dust PSD, as well as saltation PSD, also depends on ABL stability. This finding is consistent  
469 with the results of Khalfallah et al. (2020). Dust PSD is dependent on ABL stability for ~~three reasons. First, under similar~~  
470 ~~mean wind conditions, the mean surface shear stress is larger in unstable than in stable conditions. Second~~ two reasons. First,  
471  $u_*$  is a stochastic variable and the PDF of  $u_*$  profoundly influences the magnitude of saltation flux,  $Q$ , because of the non-  
472 linear relationship between  $Q$  and  $u_*$ . With fixed  $u_*$  mean, a larger  $u_*$  variance corresponds to a larger  $Q$ . Unstable ABL has  
473 in general larger  $u_*$  variances which generate stronger saltation bombardment and produce the emission of finer dust particles.  
474 ~~Third~~ Second, in unstable ABL, turbulence is generally stronger and in strong turbulent flows, the proportion of saltation  
475 particles with large impacting kinetic energy is larger than in weak turbulent flows. Consequently, saltation in unstable  
476 ABLs is more fully developed and saltation bombardment has higher intensity.

477 The dependencies of dust PSD on  $u_*$  and ABL stability are ultimately attributed to the statistic ~~behavior~~ behaviour of  $u_*$ ,  
478 i.e., its PDF  $p(u_*)$ , or more simply its mean and variance. These dependencies point to the same fact that, for a given soil,  
479 saltation bombardment plays ~~the~~ a determining role for the dust PSD. Stronger saltation causes the emission of finer dust.

480 The dependency of dust PSD on  $u_*$  and ABL stability is made complicated by soil surface condition. In the case of strong  
481 saltation and very weak surface binding, the dust PSD dependency on  $u_*$  may become less obvious. In the case of strong  
482 surface binding, dust emission in certain size ranges may be prohibited.

483  
484 *Data availability.* Data can be accessed by contacting the corresponding authors.  
485

486 *Author contributions.* Yaping Shao performed the data analyses and ~~wrote~~drafted the manuscript. Jie Zhang and Ning Huang  
487 contributed to the conception of the study ~~and helped perform~~, the data analysis ~~with constructive discussions and the~~  
488 writing of the manuscript. Masahide Ishizuka, Masao Mikami and John Leys conceived, designed and performed the  
489 experiments ~~and helped finalize the paper~~.

490  
491 *Competing interests.* The authors declare that they have no conflict of interest.

492  
493 *Acknowledgments.* We thank the National Key Research and Development Program of China (2016YFC0500901), the  
494 National Natural Foundation of China (11602100, 11172118) and the Fundamental Research Funds for the Central  
495 Universities (lzujbky-2020-cd06) for support. The JADE project was supported by Kakenhi, Grants-in-Aid for Scientific  
496 Researches (A) from the Japan Society for the Promotion of Science (Nos. 17201008 and 20244078) and the Lower Murray-  
497 Darling Catchment Management Authority. We are grateful to the three referees for their constructive comments and to Dr.  
498 Sylvain Dupont and Dr. Jasper Kok for helpful discussions.

## 499 **References**

- 500 [Albani, S., Mahowald, N. M., Perry, A. T., Scanza, R. A., Zender, C. S., Heavens, N. G., Maggi, V., Kok, J. F. and Otto-](#)  
501 [Bliesner, B. L., Improved dust representation in the Community Atmosphere Model. \*J. Adv. Model. Earth Syst.\*, 6: 541–](#)  
502 [570, doi:10.1002/2013MS000279, 2014.](#)
- 503 Alfaro, S. C., Gaudichet, A., Gomes, L. and Maille, M., Modeling the size distribution of a soil aerosol produced by  
504 sandblasting. *J. Geophys. Res-Atmos.*, 102: 11239-11249, <https://doi.org/10.1029/97JD00403>, 1997.
- 505 Astrom, J. A., Statistical models of brittle fragmentation. *Adv. Phys.*, 55: 247-278. <https://doi.org/10.1080>  
506 [/00018730600731907](https://doi.org/10.1080/00018730600731907), 2006.
- 507 Businger, J. A., Wyngaard, J. C., Izumi, J. and Bradley, E. F., Flux-Profile Relationships in the Atmospheric Surface Layer,  
508 *J. Atmospheric Sci.*, 28(2): 181–189. [https://doi.org/10.1175/1520-0469\(1971\)028<0181:FPRITA>2.0.CO;2](https://doi.org/10.1175/1520-0469(1971)028<0181:FPRITA>2.0.CO;2), 1971.
- 509 [Csanady \(1963, Turbulent Diffusion of Heavy Particles in the Atmosphere. \*J. Atmos. Sci.\* 20, 201–208\).Csanady, G. T.,](#)  
510 [Turbulent Diffusion of Heavy Particles in the Atmosphere. \*J. Atmos. Sci.\*, 20: 201–208, https://doi.org/10.1175/1520-](#)  
511 [0469\(1963\)020<0201:TDOHPI>2.0.CO;2, 1963.](#)
- 512 [Dupont, S., Scaling of dust flux with friction velocity: time resolution effects. \*J. Geophys. Res-Atmos.\*, 125, e2019JD031192,](#)  
513 <https://doi.org/10.1029/2019JD031192>, 2020.
- 514 [Durána, O., Andreotti, B. and Claudin, P., Numerical simulation of turbulent sediment transport, from bed load to](#)  
515 [saltation. \*Physics of Fluids\*, 24\(10\): 709-737, https://doi.org/10.1063/1.4757662, 2012.](#)

516 [Gillette, D. A., Blifford, I. H. and Fenster, C. R., Measurements of aerosol size distributions and vertical fluxes of aerosols](#)  
517 [on land subject to wind erosion. J. Appl. Meteor., 11: 977-987, <https://doi.org/10.1175/1520->](#)  
518 [0450\(1972\)011<0977:MOASDA>2.0.CO;2, 1972.](#)

519 Gillette, D. A., Blifford, I. H. and Fryrear, D. W., Influence of wind velocity on size distributions of aerosols generated by  
520 wind erosion of soils. J. Geophys. Res., 79: 4068-4075. <https://doi.org/10.1029/JC079i027p04068>, 1974.

521 Gillette, D. A., Production of dust that may be carried great distances. Geol. Soc. Am., 186, 11 – 26.  
522 <https://doi.org/10.1130/SPE186-p11>, 1981.

523 [Giorgi, F., Coppola, E., Solmon, F., Mariotti, L., Sylla, M. B., Bi, X., Elguindi, N., Diro, G. T., Nair, V., Giuliani, G.,](#)  
524 [Turuncoglu, U. U., Cozzini, S., Güttler, I., O'Brien, T. A., Tawfik, A. B., Shalaby, A., Zahey, A. S., Steiner, A. L., Stordal,](#)  
525 [F., Sloan, L. C. and Brankovic, C., RegCM4: model description and preliminary tests over multiple CORDEX domains.](#)  
526 [Clim. Res., 52, 7–29. doi: 10.3354/cr01018, 2012.](#)

527 Ishizuka, M., Mikami, M., Leys, J. F., Yamada, Y., Heidenreich, S., Shao, Y. and McTainsh, G. H., Effects of soil moisture  
528 and dried raindroplet crust on saltation and dust emission. J. Geophys. Res-Atmos., 113: D24212. <https://doi.org/10.1029/>  
529 [2008JD009955](#), 2008.

530 Ishizuka, M., Mikami, M., Leys, J. F., Shao, Y., Yamada, Y. and Heidenreich, S., Power law relation between size-resolved  
531 vertical dust flux and friction velocity measured in a fallow wheat field. Aeolian Research, 12: 87–99,  
532 <https://doi.org/10.1016/j.aeolia.2013.11.002>, 2014.

533 Kaimal, J. C. and Finnigan J. J., Atmospheric Boundary Layer Flows: Their Structure and Measurements. Bound.-Lay.  
534 Meteorol., 72: 213–214. <https://doi.org/10.1007/BF00712396>, 1995.

535 Khalfallah, B., Bouet, C., Labiadh, M., Alfaro, S., Bergametti, G., Marticorena, B., Lafon, S., Chevaillier, S., Féron, A.,  
536 Hease, P., Henry-des-Tureaux, T., Sekrafi, S., Zapf, P. and Rajot, J. L., Influence of atmospheric stability on the size-  
537 distribution of the vertical dust flux measured in eroding conditions over a flat bare sandy field. J. Geophys. Res-Atmos.,  
538 125, e2019JD031185. <https://doi.org/10.1029/2019JD031185>, 2020.

539 [Klose, M. and Shao, Y., Stochastic parameterization of dust emission and application to convective atmospheric conditions.](#)  
540 [Atmos. Chem. Phys., 12\(1\): 3263-3293, <https://doi:10.5194/acp-12-7309-2012>, 2012.](#)

541 [Klose, M., Shao, Y., Li, X., Zhang, H., Ishizuka, M., Mikami, M. and Leys, J. F., Further development of a parameterization](#)  
542 [for convective turbulent dust emission and evaluation based on field observations. J. Geophys. Res-Atmos., 119: 10,441–](#)  
543 [10. <https://doi.org/10.1002/2014JD021688>, 2014.](#)

544 Kok, J. F., Does the size distribution of mineral dust aerosols depend on the wind speed at emission? Atmos. Chem. Phys.,  
545 11: 10149-10156. <https://doi.org/10.5194/acp-11-10149-2011>, 2011a.

546 Kok, J. F., A scaling theory for the size distribution of emitted dust aerosols suggests climate models underestimate the size  
547 of the global dust cycle. Proc. Natl. Acad. Sci. USA, 108(3): 1016-1021. <https://doi.org/10.1073/pnas.1014798108>,  
548 2011b.

549 [Kok, J. F., Parteli, E. J., Michaels, T. I. and Karam, D. B., The physics of wind-blown sand and dust. Reports on Progress in](#)  
550 [Physics Physical Society, 75\(10\): 106901. <https://doi.org/10.1088/0034-4885/75/10/106901> , 2012.](#)

551 [Laurent, B., Marticorena, B., Bergametti, G., Mei, F., Modeling mineral dust emissions from Chinese and Mongolian deserts.](#)  
552 [Global Planet Change, 52: 121–141. <https://doi.org/10.1016/j.gloplacha.2006.02.012>, 2006.](#)

553 Li, G., Zhang, J., Herrmann, H. J., Shao, Y. and Huang, N. Study of Aerodynamic Grain Entrainment in Aeolian Transport,  
554 Geophys. Res. Lett., [47\(11\)](#). <https://doi.org/10.1029/2019GL086574>, 2020.

555 [Liu, D., Ishizuka, M., Mikami, M., ~~Li, H.~~ and Shao, Y., Turbulent characteristics of saltation and uncertainty of saltation](#)  
556 [model parameters, Atmos. Chem. Phys., 18: 7595–7606. <https://doi.org/10.5194/acp-18-7595-2018>, 2018.](#)

557 [Lu, H., and Shao, Y., A new model for dust emission by saltation bombardment. J. Geophys. Res-Atmos., 104,:](#) 16827-  
558 16842. <https://doi.org/10.1029/1999JD900169>, 1999.

559 [Marticorena, B., Bergametti, G., Aumont, B., Callot, Y., N’Doume, C. and Legrand, M., Modeling the atmospheric dust](#)  
560 [cycle: 2. Simulation of Saharan dust sources. J. Geophys. Res., 102D\(4\): 4387–4404,](#)  
561 <https://doi.org/10.1029/96JD02964>, 1997.

562 [Martin, R. L. and Kok, J.F., Wind-invariant saltation heights imply linear scaling of aeolian saltation flux with shear stress.](#)  
563 [Science Advances, Vol. 3, no. 6, e1602569, DOI: 10.1126/sciadv.1602569, 2017.](#)

564 Mikami, M., Yamada, Y., Ishizuka M., Ishimaru, T., Gao, W. and Zeng, F., Measurement of saltation process over gobi and  
565 sand dunes in the Taklimakan desert, China, with newly developed sand particle counter. J. Geophys. Res-Atmos., 110,  
566 D18S02, <https://doi.org/10.1029/2004JD004688>, 2005.

567 Owen, R. P., Saltation of uniform grains in air. J. Fluid. Mech., 20,:

568 225–242, <https://doi.org/10.1017/S0022112064001173>,  
1964.

569 Pisso, I., Sollum, E., Grythe, H., Kristiansen, N., Cassiani, M., Eckhardt, S., Arnold, D., Morton, D., Thompson, R. L.,  
570 Groot Zwaafink, C. D., Evangelizou, N., Sodemann, H., Haimberger, L., Henne, S., Brunner, D., Burkhardt, J. F.,  
571 Fouilloux, A., Brioude, J., Philipp, A., Seibert, P., and Stohl, A., The Lagrangian particle dispersion model FLEXPART  
572 version 10.4. Geosci. Model Dev., 12,:

573 4955–4997, <https://doi.org/10.5194/gmd-12-4955-2019>, 2019.

574 [Reid, J., Raupach, M.R., Drag and drag partition on rough surfaces. Boundary-Layer Meteorol., 60, 375–395.](#)  
575 <https://doi.org/10.1007/BF00155203>, 1992.

576 [Reid, J. S., Reid, E. A., Walker, A., Piketh, S., Cliff, S., Al Mandoos, A., Tsay,](#)  
577 [S.-C. and Eck, T. F., Dynamics of southwest Asian dust particle size characteristics with implications for global dust](#)  
578 [research. J. Geophys. Res-Atmos., 113, D14212. <https://doi.org/10.1029/2007JD009752>, 2008.](#)

579 Rice, M. A., Willetts, B. B. and McEwan, I. K., An experimental study of multiple grain-size ejecta produced by collisions  
580 of saltating grains with a flat bed. Sedimentology, 42,:

581 695-706. <https://doi.org/10.1111/j.1365-3091.1995.tb00401.x>, 1995.

582 Rice, M. A., Willetts, B. B. and McEwan, I. K., Observations of collisions of saltating grains with a granular bed from high-  
speed cine-film. Sedimentology, 43,:

21-31. <https://doi.org/10.1111/j.1365-3091.1996.tb01456.x>, 1996.

Rosenberg, P. D., Parker, D. J., Ryder, C. L., Marsham, J. H., Garcia-Carreras, L., Dorsey, J. R., Briks, I. M., Dean A. R.,  
Crosier J., McQuaid, J. B. and Washington, R., Quantifying particle size and turbulent scale dependence of dust flux in the

583 | Sahara using aircraft measurements, *J. Geophys. Res-Atmos.*, 119; 7577–7598. <https://doi.org/10.1002/2013JD021255>,  
584 | 2014.

585 | [Shao, Y., A model for mineral dust emission. \*J. Geophys. Res-Atmos.\*, 106: 20239-20254. https://doi.org/10.1029/  
586 | 2001JD900171, 2001.](https://doi.org/10.1029/2001JD900171)

587 | [Shao, Y., Simplification of a dust emission scheme and comparison with data. \*J. Geophys. Res.\*, 109,  
588 | <https://doi.org/10.1029/2003JD004372>, 2004.](https://doi.org/10.1029/2003JD004372)

589 | [Shao, Y., \*Physics and Modelling of Wind Erosion\*. Springer, https://doi.org/10.1007/978-1-4020-8895-7, 2008.](https://doi.org/10.1007/978-1-4020-8895-7)

590 | [Shao, Y., Ishizuka, M., Mikami, M. and Leys, J. F., Parameterization of size-resolved dust emission and validation with  
591 | measurements. \*J. Geophys. Res.-Atmos.\*, 116, D08203, <https://doi.org/10.1029/2010JD014527>, 2011.](https://doi.org/10.1029/2010JD014527)

592 | [Shao, Y. and Mikami, M., Heterogeneous Saltation: Theory, Observation and Comparison. \*Boundary-Layer  
593 | Meteorol.\*, 115: 359–379, <https://doi.org/10.1007/s10546-004-7089-2>, 2005.](https://doi.org/10.1007/s10546-004-7089-2)

594 | Shao, Y., Raupach, M. R. and Findlater, P. A., Effect of saltation bombardment on the entrainment of dust by wind. *J.*  
595 | *Geophys. Res.-Atmos.*, 98; 12719-12726. <https://doi.org/10.1029/93JD00396>, 1993.

596 | [Sow, M., Alfaro, S., Rajot, J. L., Marticorena, B., Size resolved dust emission fluxes measured in Niger during 3 dust storms  
597 | of the AMMA experiment. \*Atmos. Chem. Phys.\*, 9, 3881-3891, <https://doi.org/10.5194/acp-9-3881-2009>, 2009.](https://doi.org/10.5194/acp-9-3881-2009)

598 | [Sterk G., Jacobs A.F.G. and van Boxel J.H., The effect of turbulent flow structures on saltation sand transport in the  
599 | atmospheric boundary layer. \*EARTH SURF. PROC. LAND.\*, 23: 877 - 887, \[https://doi.org/10.1002/\\(SICI\\)1096-  
600 | 9837\\(199810\\)23:10<877::AID-ESP905>3.0.CO;2\]\(https://doi.org/10.1002/\(SICI\)1096-<br/>600 | 9837\(199810\)23:10<877::AID-ESP905>3.0.CO;2\)-Shao, Y., A model for mineral dust emission, 1998.](https://doi.org/10.1002/(SICI)1096-9837(199810)23:10<877::AID-ESP905>3.0.CO;2)

601 | [Stout, J.E., Zobeck, T.M., Intermittent saltation. \*Sedimentology\*, 44: 959–970, \[https://doi.org/10.1046/j.1365-  
602 | 3091.1997.d01-55.x\]\(https://doi.org/10.1046/j.1365-<br/>602 | 3091.1997.d01-55.x\), 1997.](https://doi.org/10.1046/j.1365-3091.1997.d01-55.x)

603 | ~~[J. Geophys. Res-Atmos., 106, 20239-20254., 2001.](https://doi.org/10.1029/2001JD900171)~~

604 | Stull, R. B., *An Introduction to Boundary Layer Meteorology*. Kluwer Academic Publishers, Boston.  
605 | <http://dx.doi.org/10.1007/978-94-009-3027-8>, 1988.

606 | [Ungar, J.E. and Haff, P.K., Steady state saltation in air. \*Sedimentology\*, 34: 289–299, \[https://doi.org/10.1111/j.1365-  
607 | 3091.1987.tb00778.x\]\(https://doi.org/10.1111/j.1365-<br/>607 | 3091.1987.tb00778.x\), 1987.](https://doi.org/10.1111/j.1365-3091.1987.tb00778.x)

608 | [Walklate, P.J., A random-walk model for dispersion of heavy particles in turbulent air flow. \*Boundary-Layer  
609 | Meteorol\* 39: 175–190, <https://doi.org/10.1007/BF00121873>, 1987.](https://doi.org/10.1007/BF00121873)

610 | [Wang, L., and D. E. Stock, Dispersion of Heavy Particles by Turbulent Motion. \*J. Atmos. Sci.\*, 50: 1897–  
611 | 1913, \[https://doi.org/10.1175/1520-0469\\(1993\\)050<1897:DOHPBT>2.0.CO;2\]\(https://doi.org/10.1175/1520-0469\(1993\)050<1897:DOHPBT>2.0.CO;2\), 1993.](https://doi.org/10.1175/1520-0469(1993)050<1897:DOHPBT>2.0.CO;2)

612 | [Webb, N. P., Chappell, A., LeGrand, S. L., Ziegler, N. P., Edwards, B. L., A note on the use of drag partition in aeolian  
613 | transport models. \*Aeolian Research\*, 42, <https://doi.org/10.1016/j.aeolia.2019.100560>, 2020.](https://doi.org/10.1016/j.aeolia.2019.100560)

614 | Yahaya, S., Frangi, J. P. and Richard, D. C., Turbulent characteristics of a semiarid atmospheric surface layer from cup  
615 | anemometers - Effects of soil tillage treatment (Northern Spain). *Annales Geophysicae*, 21: 2119-2131.  
616 | <https://doi.org/10.5194/angeo-21-2119-2003>, 2003.



617 | [Zender, C.S., Bian, H., Newman, D., Mineral Dust Entrainment and Deposition \(DEAD\) model: Description and 1990s dust](#)  
618 | [climatology. J. Geophys. Res., 108: 4416, <https://doi.org/10.1029/2002JD002775>, 2003.](#)